
Effect of mix design inputs, curing and compressive strength on the durability of $Na_2SO_4$-activated high volume fly ash concretes


Diego F. Velandia, Cyril J. Lynsdale, John L. Provis, Fernando Ramirez



PII: S0958-9465(17)30954-X

DOI: 10.1016/j.cemconcomp.2018.03.028

Reference: CECO 3036

To appear in: *Cement and Concrete Composites*

Received Date: 26 October 2017

Revised Date: 20 February 2018

Accepted Date: 31 March 2018

Please cite this article as: D.F. Velandia, C.J. Lynsdale, J.L. Provis, F. Ramirez, Effect of mix design inputs, curing and compressive strength on the durability of $Na_2SO_4$-activated high volume fly ash concretes, *Cement and Concrete Composites* (2018), doi: 10.1016/j.cemconcomp.2018.03.028.

# Effect of mix design inputs, curing and compressive strength on the durability of $Na_2SO_4$-activated high volume fly ash concretes

**Diego F. Velandia[a,b*], Cyril J. Lynsdale[a], John L. Provis[c], Fernando Ramirez[d]**

[a]Department of Civil and Structural Engineering, University of Sheffield, Sir Frederick Mappin Building, Mappin Street, Sheffield, S13JD, UK
[b]Research and Development, Argos, Carrera 62 No. 19 - 04 , Bogotá, Colombia
[c]Department of Materials Science and Engineering, University of Sheffield, Sir Robert Hadfield Building, Mappin Street, Sheffield, S13JD, UK
[d]Department of Civil and Environmental Engineering, Universidad de los Andes, Carrera 1 este No. 19A-40, Edificio Mario Laserna, Oficina ML 632, Bogotá, Colombia

## ABSTRACT

This paper aims to advance research on the use in concrete of a high volume of fly ash, with a high loss on ignition value, aiding in sustainable low carbon footprint construction. To this end, the work explores the benefits that may be achieved in terms of long-term concrete performance from the incorporation of fly ash along with a chemical activator. Durability tests are performed on concrete with an activated hybrid cementitious system: Portland cement (PC) and high volume fly ash with sodium sulfate. The chloride diffusion coefficient significantly decreased over time for the activated system (50% PC - 50% fly ash with added sodium sulfate) compared to the control samples (100% PC and 80% PC - 20% fly ash) at the same water to cementitious material ratio. This behavior is particularly evident in samples cured under controlled laboratory conditions (100% RH and 23°C). However, outdoor curing increases the permeability for all concretes. Long term carbonation is also investigated under natural exposure conditions, and samples that are cured outdoors exhibit a significant carbonation depth. The compressive strength is correlated with the durability parameters: the durability performance improves as the compressive strength increases, indicating that as is the case for Portland cement (but not always for alkali-activated binders), the microstructural factors which yield high strength are also contributing to durability properties.

**Keywords:** concrete durability; alkali-activated hybrid cement; high volume fly ash; sodium sulfate; loss on ignition

## 1. INTRODUCTION

Studies using high volume fly ash with both Portland cement and alkaline activators are not yet numerous, although investigations have focused on the strength evolution of mortar and concrete **[1-3]**. The main present challenges are related to curing temperature, setting time delay, low early strength evolution and durability **[4]**. As mentioned in a recent RILEM report **[5]**, mixes including alkali activators need more research in terms of shrinkage, carbonation, long term performance and alkali aggregate reactions.

Considering the importance of studying the durability of $Na_2SO_4$-activated high volume fly ash concretes, it is important to first understand the concept of concrete deterioration, which depends on the permeability of the material. Gases, ions and liquids penetrate the material, reacting with concrete constituents and affecting the material properties. Matrix deterioration can occur due to physical and chemical processes **[6-8]**. In most cases, water or chemical species dissolved in water are the causes of concrete durability problems **[9]**. Pores present in the matrix (aggregates, cement paste–aggregate interfaces and cement paste) affect the mechanical properties of concrete, such as the strength and modulus of elasticity **[8]**. Different liquids, gases and ions can penetrate concrete and move inside the matrix due to absorption, permeability and diffusion **[7]**. These processes depend on physicochemical gradients, such as pressure, concentration, temperature, and humidity, as well as any applied voltage.

Absorption occurs due to capillary forces in a non-saturated concrete **[10]**; water at the surface enters the structure and fills available pores depending on the concrete moisture content. Permeability is related to how easily a fluid passes through a matrix due to a pressure gradient. Considering the effects of different parameters that affect the water permeability of concrete, this parameter can often be correlated to compressive strength. In general, when strength increases, the water permeability decreases **[11, 12]**, as both are related to the microstructural development of the material. Diffusion which occurs due to a chemical potential or a concentration gradient **[9]**; ions will move from areas of high to low concentration **[13]**, controlled by the capillary pore size, concentration gradient and cementitious material composition.

Water absorption of concrete generally decreases with an increase in fly ash dosage; it is correlated to permeable voids, which are reduced at later age when fly ash is included in higher proportions **[14]**. A linear correlation has been observed between the volume of penetrable pores when using absorption and sorptivity tests **[15]**. Chloride permeability as determined using the rapid chloride permeability test is reduced for high volume fly ash (HVFA) concretes at an age of 56 days **[16]**; for a HVFA concrete designed according to the mix design requirements proposed by Malhotra, the chloride permeability values usually lie in the "very low" band according to ASTM C 1202 **[14]**.

However, chloride ingress processes involving high-volume pozzolanic materials are observed to be variable, and require further investigation **[17]**. Parameters such as the type of the supplementary cementitious material, water to cementitious material ratio, cement type, curing and exposure condition affect chloride penetration. For example, for concretes with 55% to 70% fly ash, an inadequate curing regime and low fly ash fineness can increase chloride penetration **[18].** High volume fly ash concretes may perform poorly in chloride ingress tests compared to PC concretes after 28 days, whereas the performance improves after 90 days or a year **[19]**.

Carbonation of fly ash-containing concretes is also to some degree contentious due to the competition between their low portlandite content and low permeability, which has led to mixed results for different specimens described in the literature. HVFA concretes often have low permeabilities due to their low water to cementitious materials ratio (W/CM) if a suitable curing process enables the fly ash to react extensively; this may reduce carbonation depth. When low W/CM samples are water cured, they become more resistant to carbonation due to their low porosity **[20-22]**. Capillary pores are dry when the relative humidity is low and saturated when the relative humidity is high, reducing the carbonation process in both instances, meaning that carbonation is fastest at intermediate relative humidities **[23]**. However, because HVFA concretes contain less portlandite due to its consumption in pozzolanic reactions, once the $CO_2$ does enter the concrete, its contribution to slowing carbonate mass transport, by binding the carbonate as calcite is reduced **[24]**, which means that the relationship between porosity and carbonation rate changes as a function of binder chemistry. When 100% Portland cement and HVFA concretes exhibit similar porosities following different curing procedures, the latter display a higher carbonation depth at 28 days and at 1 year **[19]**.

Considering the current state of art, the main objective of this study was to investigate the durability performance of an activated hybrid cementitious concrete, with inclusion of a high volume of type F fly ash (with high loss on ignition (LOI)), and chemically activated by sodium sulfate. Mixes with 50% FA and 1% sodium sulfate were used for this study. Different durability tests were performed on samples cured in the lab and under outdoor conditions: water permeability, chloride penetration, chloride diffusion coefficient and carbonation.

## 2. MATERIALS AND METHODS

### 2.1. Materials

The materials and dosages were selected based on a study where characterization of pastes and mortars was performed using the same materials **[25]**. TP fly ash is a high LOI supplementary cementitious material, with chemical composition as presented in Table 1. The sum of $SiO_2$, $Al_2O_3$ and $Fe_2O_3$ reaches the minimum mentioned in ASTM C 618 **[26]**; the LOI value is higher than the basic limit of 6% but lower than the 12% which is given as the absolute maximum limit in ASTM C 618. The chemical composition was determined using a PANalytical Axios sequential wavelength dispersive X-ray fluorescence (XRF). The mineralogical compositions of the fly ash and Portland cement (Type III according to ASTM C150 **[27]**) are given in Table 2 and 3 respectively. The amorphous content of TP fly ash is higher than 60%. The mineralogy was evaluated by X-ray diffraction (XRD) using a PANalytical X'PERT-PRO MPD in Bragg-Brentano configuration with an X'celerator detector. The Rietveld method was used to quantify the crystalline phases via the X'Pert HighScore Plus software package. The sodium sulfate purity is 95%, and this activator was also selected based on the study of Velandia *et al.* **[25]**.

### 2.2. Concrete evaluation

Concrete designs were developed to obtain a slump of 225 mm. Three different W/CM were considered for a specified compressive strength of 28 MPa, 35 MPa and 41 MPa at 28 days for 20% FA mixes. The input parameters are shown in Table 4. All of these proportions were determined for 1 $m^3$ and adjusted to the laboratory mixer capacity. Each mix is described based on the Mix ID due to the number of parameters studied in the concrete. All of these parameters are listed in Table 5, including the water to cementitious material ratio and curing type.

The curing treatments included laboratory and outdoor ambient curing (Figure 1). Table 6 presents each concrete test and its standard, and the age of evaluation. The test used to evaluate water permeability was a Colombian standard **[29]**, which measures water penetration depth in a cylindrical specimen, with a diameter and length of 10 cm. In this test, the sample is exposed under an applied water pressure of 0.5 MPa for 4 days. After 4 days, the sample is broken using the ASTM C 496 cylinder splitting test **[33]**. Carbonation was evaluated under natural environmental conditions in Bogotá, Colombia, Figure 2. The average $CO_2$ concentration in the environment was 350 ppm, with a relative humidity of 63%, and the temperature remained between 15-20°C. Cylinders exposed to ambient carbonation were 5 cm thick and 10 cm in diameter. At the end of the exposure period, the cylinder splitting test was performed to divide the cylinder in two sections. One of the sections was sprayed with phenolphthalein to enable carbonation to be visualized.

The Minitab Multi-Vari Chart tool was used to perform part of the analysis. This Minitab tool considers a maximum of 4 variables. It analyses the variance based on the mean of each variable. Each point of each factor is the mean for each level of analysis.

## 3. RESULTS AND DISCUSSION

### 3.1. Compressive strength

Samples with W/CM of 0.557 (Figure 3a) exhibited similar behaviors when cured under different conditions, but this was not the case for samples with W/CM of 0.483 and 0.426 as seen in Figure 3b and 3c. Samples with 50% fly ash were notably affected by the curing process. Mixes with an activator that were cured in the curing room typically exhibited increased compressive strengths compared to mixes cured outside. These results are consistent with the findings of Poon *et al.* **[2]**, where the influence of the curing process on compressive strength evolution was studied using mixes with 55% fly ash and calcium sulfate as an activator; specimens were cured at 65°C for 6 hours before continuing a 27°C curing. This curing process exhibited a positive effect (70% increase in the compressive strength) compared to a control mix cured under standard conditions **[2]**. However, in another study, pastes with sodium sulfate (1% by mass of cementitious material) and 50% PC - 50% FA performed better when cured for 7 days at 20°C than when cured for the first day at 60°C and the remaining 6 days at 20°C **[3]**. Velandia *et al.* **[25]** also found that curing mixes with sodium sulfate at 23°C increased compressive strength due to portlandite consumption and ettringite formation.

As seen in Figure 3a, 3b and 3c, mixes with 1% sodium sulfate always displayed higher compressive strengths compared to mixes with 50% fly ash without an activator, consistent with results for mortars using the same cementitious materials and activator proportions **[25]**. This was also evident in the work of Qian *et al.*, who also used $Na_2SO_4$

as an activator in high volume fly ash mixes **[1]**. This activator initiates chemical reactions that increase the alkalinity, accelerates fly ash dissolution, and increases the matrix density by increasing ettringite formation.

The parameters considered in the Multi-Vari Chart include the fly ash percentage, W/CM, curing and age. Each point represents the mean of the specific level of analysis. As shown in Figure 3d, the compressive strength is significantly affected by the W/CM ratio and fly ash percentage. In general, when samples are cured in the lab, as the W/CM ratio is reduced the compressive strength increases, whereas as the fly ash content increases this parameter decreases. When samples are cured outside, the effect of W/CM is negligible compared to samples cured in the laboratory. The curing effect becomes more relevant with age; as the age is increased the gap between curing in the lab and outdoors increases. The inclusion of the activator increases the compressive strength at early age. The change in the slope when sodium sulfate is included allows identification of the positive influence of this component in the matrix. Concretes with 50% FA come closer to reaching the performance of the control samples from 90 to 360 days.

### 3.2. Water permeability

The curing process also influenced the water permeability, especially in mixes with high fly ash volumes as seen in Figure 4. Samples cured outdoors exhibited higher water permeabilities. The environment in the curing room guaranteed the availability of sufficient water to form the hydration products, while outdoor conditions, at lower relative humidity and temperature, did not. In most cases, specimens with activators exhibited lower water permeabilities than control samples after 180 days. The accelerated consumption of portlandite by activation of the fly ash from the beginning of hydration may help to reduce pores; according to Velandia *et al.* significant portlandite consumption starts to be evident at 3 days **[25]**. The effect of the W/CM ratio on water permeability was also significant for fly ash mixes.

As seen in Figure 4d, all of the input parameters significantly influence the water permeability depth. In addition, the combined effects of multiple parameters must be evaluated, as there are synergies and competitive effects between the influences of each individual parameter. For example, the final effects become relevant when the W/CM, fly ash percentage and curing type effects are combined.

## 3.3. Chloride penetration testing

According to the results presented in Figure 5, mixes with an activator and 0.557 W/CM performed better than control mixes (20%FA and 50%FA) after 180 days. These performance improvements occurred earlier for lower W/CM ratios. In comparison to mixes cured outdoors, samples with activators exhibited similar or lower charges passed in most cases.

Although the chloride penetration measurements can be decreased by increasing the fly ash percentage in HVFA concrete **[16]**, this decrease only occurs at later age and strongly depends on the W/CM level. In most cases, 50% fly ash mixes without an activator did not perform better than control samples. Some authors have suggested that the rapid chloride penetration test (which is actually measuring charge passed during the test and not movement of chloride) is not reliable for mixes with activators due to the high pore solution alkalinity and ionic strength **[34, 35]**. Charge passed depends on dissolved ions in the pore solution moving in the electric field, which changes with cement chemistry. In this case, a negative effect cannot be seen for mixes with an activator, which is likely due to low activator concentrations and low sulfate ion mobility, as based on the trends presented in Figure 5a, 5b and 5c.

On the other hand, the effect of the curing process is not clear. This is likely due to the poor precision of the test, where the standard itself **[30]** considers a maximum repeatability of 42%. Although this test is widely used in the concrete industry for quality control, additional tests must be considered to satisfactorily evaluate the concrete performance and the influence of different materials in the concrete matrix.

No significant effect of curing is evident in the multi-chart plot presented in Figure 5d. The effect of W/CM ratio is only apparent at early age; as curing time increases, the charge passed values are similar for all of the W/CM values tested. Although this behavior is similar for different fly ash percentages, the charge passed decreases with the inclusion of sodium sulfate when compared to the control sample with 50% FA.

## 3.4. Chloride migration coefficient

Based on the results presented in Figure 6, curing significantly affects the chloride migration test results of fly ash-rich concrete mixes. Generally, the 100% cement mix performed better than fly ash mixes when cured outside, but no activator effect is evident for these samples. Reinhardt and Jooss **[36]** suggested that temperature variations during the curing process affect the concrete properties, where temperature variation from 20°C to 80°C for mixes with 40% FA reduced the diffusion resistance by approximately 10-20%. As seen in Figure 2, the temperature of the environment is an average but it could vary in a range of 10°C per day.

An increase in the chloride diffusion coefficient for fly ash mixes was likely due to the absorption increase during the first days of the analysis. Ismail *et al.* noted that chloride sorption increases when fly ash is included in alkali activated binders **[37]**. Bernal *et al.* also noted a relation between the diffusion coefficient and sorptivity **[34]**.

From 90 to 180 days, activated mixes exhibited a lower diffusion coefficient ($< 7x10^{-12}$ $m^2/s$) compared to the control samples. According to Burden, the performance of high volume fly ash concrete (30%, 40% and 50%) improved after 90 days and a year, but the material was poorly performing prior to those times **[19]**. Although the improvement occurs more rapidly with an activator as seen in Figure 6a, 6b and 6c, mixes without an activator also displayed a significant improvement over time. The W/CM ratio influenced the diffusion coefficient, but only for mixes cured in the lab.

The effect of each parameter on the diffusion coefficient is summarized in Figure 6d. After 90 days, the effect of the sodium sulfate activator is positive for laboratory cured samples and negative for outdoor cured samples. A decreased W/CM ratio reduces the diffusion coefficients of most samples. In addition, the curing process has a significant impact during early times. After a year, the diffusion coefficients of the activated mixes are low, both for samples cured in the laboratory and outdoors.

### 3.5. Carbonation

This analysis only includes specimens cured outdoors, which were affected by humidity and moisture cycling and so are expected to be more subjected to carbonation processes. Humidity, dry and wet cycling, and $CO_2$ concentration variations strongly affect the carbonation depth **[38, 39]**. Carbonation had a significant impact on high volume fly ash samples. According to Figure 7a, the W/CM ratio did not significantly affect the carbonation of the high volume fly ash mixes.

Although the carbonation depth was always lower for mixes with activator at 90 days compared to mixes with 50% FA without activator, no significant difference can be distinguished between them. Carbonation depths for mixes with 20% fly ash did not significantly change over time as the 50% fly ash mixes did. The average relative humidity in this study was between 50% and 70%, which according to Wierig and Saeki *et al*. **[21, 22]** is an optimum range for carbonation. Another factor affecting carbonation is the low portlandite content in mixes with 50% fly ash as shown in the study of Younsi, resulting in faster carbonation compared to 100% cement concretes **[20]**; the reduction in concrete permeability for 50% fly ash mixes did not give a corresponding carbonation reduction compared to mixes with 0% and 20% FA. It is possible that the controlling parameter was actually the PC content, rather than the total cementitious materials content, as proposed by Ho and Lewis **[40]**.

The inclusion of sodium sulfate reduced carbonation levels compared to samples with 50% fly ash, probably because the differences in the porosity of the microstructure **[25]**. The effect of the W/CM ratio is not clear. The carbonation coefficient calculated with Tutti's model **[41]** is constant at different ages for each fly ash replacement level, as shown in Figure 7b.

### 3.6. Parameters influencing concrete durability

According to Figure 8a, the water permeability decreases for 50% fly ash when an activator is used. For the same compressive strength, the water permeability decreases as the fly ash level increases. Although the compressive strength is higher for samples with 0% FA and 20% FA at the same W/CM ratio, the micro-structure of fly ash samples with 50% FA is less permeable due to the reduction of the $Ca(OH)_2$ content, as this is replaced by C-(A)-S-H through the pozzolanic reaction **[25]**. For the case of lab curing, a 20 mm water permeability depth was achieved for a strength of approximately 50 MPa in a mix with 100% cement, or for a 30 MPa strength in a 50% FA mix with 1% sodium sulfate. Under this scenario, water permeability is more directly predictive than compressive strength in terms of the other durability parameters.

Based on the results of this work, the parameters that influence the chloride penetration are defined and presented in Figure 8b. Thus, the proposed correlations depend on the compressive strength and fly ash replacement. The same chloride penetration value can be obtained for various compressive strengths depending on the fly ash replacement and sodium sulfate inclusion in the matrix. Mixes with high fly ash replacements and lower compressive strengths compared to control mixes (0% FA and

20% FA) are in the “Very Low” chloride penetration range, according to ASTM C 1202. This pattern was similar to the water permeability results. The inclusion of sodium sulfate positively affects the chloride penetration measurements, with low values measured for moderate compressive strengths.

The variations in diffusion coefficient are associated with the compressive strength and fly ash content variations. If the cementitious material type is held constant (with or without sodium sulfate), the diffusion coefficient decreases as the compressive strength increases. When the fly ash content increases and sodium sulfate is included, the diffusion coefficient decreases at constant compressive strength. This behavior is illustrated in Figure 8c. For example, a chloride diffusion coefficient of 4 $x10^{-12}$ $m^2/s$ in a 0% FA mix can be produced at a compressive strength of 80 MPa, while the same diffusion coefficient can be produced in a 50% FA and sodium sulfate mix at an approximately 40 MPa compressive strength. A similar pattern is seen in the charge passed results, where charge passed values of 500 coulombs are reached at 80 MPa without FA, or at 40 MPa in the activated 50% FA mix.

Concretes with high volume fly ash and sodium sulfate, based on the results achieved in this study, can comply with specifications for concrete used in structures exposed to sea water. For instance, in the Colombian coastal zones different ports have been built in recent years and one of the key concrete specification requirements has been a diffusion coefficient lower than $10x10^{-12}$ $m^2/s$. The results and correlations developed in this work become particularly relevant when considering the possibility of moving from prescriptive to performance based specifications **[42]**. In this case it is relevant to use these values to model service life, and to compare the predicted results with lab and on-site trials. Therefore, these new activated systems, where the performance is advantageous, can be implemented in future structures under such specifications.

## 4. CONCLUSIONS

The water permeabilities and chloride diffusion coefficients of fly ash and sodium sulfate mixes were either comparable or superior to those of control concretes with the same W/CM when water cured. Outdoor curing adversely affected the performance of the fly ash concretes. Reducing the W/CM ratio also decreased the water permeability and diffusion coefficient. The carbonation rates were not favorable for mixes with sodium sulfate.

The water permeability, chloride penetration and diffusion coefficient show some correlation with the compressive strength and fly ash percentage for indoor and outdoor cured samples. In general, the concrete behavior improved based on these parameters when the compressive strength and fly ash percentage increased and an efficient curing process was applied. Among concretes with the same compressive strength, different fly ash percentages and the same curing, lower water permeability, chloride penetration and diffusion coefficient values were observed for samples with the highest fly ash contents. When sodium sulfate is included, concrete performance improved compared to corresponding concretes without an activator.

The observed trends in durability-related parameters (water permeability, chloride penetration and diffusion coefficient) are not similar for concrete carbonation. An increased fly ash percentage increases the carbonation depth. While concrete with sodium sulfate exhibits a lower carbonation coefficient compared to control concrete with 50% FA, it exhibits high values compared to 0% FA and 20% FA concretes.

The results of this study, where different mixes including $Na_2SO_4$-activated high volume fly ash concretes have been evaluated, could be used to explore performance-based specifications. For new sustainable materials to be used in construction, performance specifications become an alternative to traditional prescriptive codes, enabling materials to be specified for sustainability and to increase service life of the structures. For instance, the results from these concretes with high volumes of moderate quality fly ash and low doses of sodium sulfate indicate that they could potentially be used for structures exposed to sea water.

**ACKNOWLEDGEMENTS**

This work was part of a PhD research program conducted at the University of Sheffield, funded by Argos (cement and concrete producer). Cement, fly ash and aggregates were supplied by this company, and admixtures by Sika Colombia. Argos' laboratory facilities were used to characterize materials and evaluate all the mix combinations. The participation of JLP was supported in part by the Engineering and Physical Sciences Research Council (UK), under grant EP/M003272/1. CJL's participation was supported in part by the Royal Academy of Engineering / The Leverhulme Trust Senior Research Fellowship.

**REFERENCES**

1. Qian J, Shi C, Wang Z. Activation of blended cements containing fly ash. Cem Concr Res 2001;31:1121-27.
2. Poon C, Kou S, Lam L, Lin Z. Activation of fly ash/cement using calcium sulfate anhydrite ($CaSO_4$). Cem Concr Res 2001;31:873-81.
3. Owens KJ, Bai Y, Cleland D, Basheer PAM, Kwasny J, Sonebil M, Taylor S, Gupta A. Activation of high volume fly Ash pastes using chemical activators. In: Second International Conference on Sustainable Construction Materials and Technologies, Universita Politecnica delle Marche, Ancona, Italy. 2010; 1759-70.
4. Shi C, Fernández Jimenez A, Palomo A. New cements for the 21st century: The pursuit of an alternative to Portland cement. Cem Concr Res 2011;41:750-763.
5. Provis JL, Van Deventer JSJ, Alkali-Activated Materials: State-of-the-Art Report, RILEM TC 224-AAM. RILEM/Springer, Dordrecht, 2014.
6. Mehta PK, Gerwick BC. Physical causes of concrete deterioration. Concr Int 1982;4:45-51.
7. Long AE, Henderson GD, Montgomery FR. Why assess the properties of near-surface concrete? Constr Build Mater 2001;15:65-79.
8. Basheer L, Kropp J, Cleland D. Assessment of the durability of concrete from its permeation properties: a review. Constr Build Mater 2001;15:93-103.
9. Claisse PA. Transport properties of concrete. Concr Int 2005; 27:43-48.
10. Bentz DP, Clifton JR, Ferraris CF, and Garboczi EJ. Transport Properties and Durability of Concrete: Literature Review and Research Plan, NISTIR 6395, U.S. Department of Commerce, Gaithersburg, MD, USA. 1999.
11. Armaghani JM, Larsen TJ, Romano DC. Aspects of concrete strength and durability. Transp Res Record 1992;1335:63-69.
12. Khatri RP, Sirivivatnanon V. Methods of deterioration of water permeability of concrete. ACI Mater. J. 1997;94:1105-1114.
13. Martys N. Survey of concrete transport properties and their measurement. National Institute of Standards and Technology. U.S. Department of Commerce. Gaithersburg, MD, USA. 1995.

14. Dinakar P, Babu K, Santhanam M. Durability properties of high volume fly ash self compacting concretes. Cem Concr Compos 2008;30:880-86.
15. Sahmaran M, Yaman I, Tokyay M. Transport and mechanical properties of self consolidating concrete with high volume fly ash. Cem Concr Compos 2009; 31:99-106.
16. Velandia D, Echeverri W. Concreto expuesto a diferentes ataques en Colombia. Noticreto 2010; 102:32-35.
17. Shi X, Xie N, Fortune K, Gong J. Durability of steel reinforced concrete in chloride environments: An overview. Constr Build Mater 2012;30:125-38.
18. Özbay E, Karahan O, Lachemi M, Hossain KMA, Atiş CD. Investigation of properties of engineered cementitious composites incorporating high volumes of fly ash and metakaolin. ACI Mater J 2012; 109:565-71.
19. Burden D. The durability of concrete containing high levels of fly ash. Thesis (MSc). University of New Brunswick, Canada. 2006.
20. Younsi A, Turcry P, Roziere E, Aït-Mokhtar A, Loukili A. Performance-based design and carbonation of concrete with high fly ash content. Cem Concr Compos 2011; 33:993-1000.
21. Wierig H. Long time studies on the carbonation of concrete under normal outdoor exposure. RILEM Seminar, Hanover, Germany. 1984
22. Saeki T, Ogha H, Nagataki S. Mechanism of carbonation and prediction of carbonation process of concrete. Concrete Library of JSCE 1991; 12:23-36.
23. Thiery M, Villain G, Dangla P, Platret G. Investigation of the carbonation front shape on cementitious materials: effects of the chemical kinetics. Cem Concr Res 2007; 37:1047-58.
24. Papadakis VG, Vayenas CG, Fardis MN. A reaction engineering approach to the problem of concrete carbonation. AIChE J 1989; 35:1639-50.
25. Velandia DF, Lynsdale CJ, Provis JL, Ramirez F, Gomez AC. Evaluation of activated high volume fly ash systems using $Na_2SO_4$, lime and quicklime in mortars with high loss on ignition fly ashes. Constr Build Mater 2016;128:248-55.
26. ASTM C 618 – 08. Standard Specification for Coal Fly Ash and Raw or Calcined Natural Pozzolan for Use in Concrete. ASTM International, West Conshohocken, PA, USA, 2008.
27. ASTM C 150/C 150M – 09. Standard Specification for Portland Cement. ASTM International, West Conshohocken, PA, USA, 2009.

28. ASTM C 39/C 39 M – 09. Standard Test Method for Compressive Strength of Cylindrical Concrete Specimens. ASTM International, West Conshohocken, PA, USA, 2009.
29. NTC 4483. Método de ensayo para determinar la permeabilidad del concreto al agua. Norma Técnica Colombiana, ICONTEC. Bogotá, Colombia, 1998.
30. ASTM C 1202 – 10. Standard Test Method for Electrical Indication of Concrete's Ability to Resist Chloride Ion Penetration. ASTM International, West Conshohocken, PA, USA, 2010.
31. NT BUILD 492. Concrete, Mortar and Cement-Based Repair Materials: Chloride Migration Coefficient from Non-Steady-State Migration Experiments. Nordtest Method. Espoo, Finland, 1999.
32. BS EN 14630:2006 Products and Systems for the Protection and Repair of Concrete Structures. Test Methods. Determination of Carbonation Depth in Hardened Concrete by the Phenolphthalein Method London, British Standards Institution. 2006.
33. ASTM C 496/C 496M – 04. Standard test method for splitting tensile strength of cylindrical concrete specimens. ASTM International, West Conshohocken, PA, USA, 2004.
34. Bernal SA, Mejía de Gutierrez R, Provis JL. Engineering and durability properties of concretes based on alkali-activated granulated blast furnace slag/metakaolin blends. Constr Build Mater 2012; 33:99-108.
35. Puertas F, Fernández-Jimenez A, Blanco-Varela MT. Pore solution in alkali-activated slag cement pastes. Relation to the composition and structure of calcium silicate hydrate. Cem Concr Res 2004; 34:139-48.
36. Reinhardt HW, Jooss M. Permeability, diffusion and capillary absorption of concrete at elevated temperature in the service range. Otto-Graf-Journal 1998;9:34-47.
37. Ismail I, Bernal SA, Provis JL, San Nicolas R, Brice DG, Kilcullen AR, Hamdan S, Van Deventer JSJ. Influence of fly ash on the water and chloride permeability of alkali-activated slag mortars and concretes. Constr Build Mater 2013; 48:1187-201.
38. Castellote M, Fernandez L, Andrade C, Alonso C. Chemical changes and phase analysis in carbonated OPC paste at different $CO_2$ concentrations. Mater Struct 2009; 42:515-25.
39. Parrot LJ. Design for avoiding damage due to carbonation-induced corrosion. ACI Special Publication 1994; 145:283-298.

40. Ho DWS, Lewis RK. Carbonation of concrete and its prediction. Cem Concr Res 1987; 17:489-504.
41. Tutti K. Service life of structures with regard to corrosion of embedded steel. ACI Special Publication 1980; 65:223-236.
42. Alexander M, Thomas M. Service life prediction and performance testing – Current developments and practical applications. Cem Concr Res 2015; 78:155-164.

**Figure captions**

Fig. 1. Curing conditions: a) Curing room, b) Outdoor curing (Bogotá, Colombia)

Fig. 2. Variation of ambient conditions: temperature, relative humidity, heat index, evaporation point, wind speed, $CO_2$ concentration

Fig. 3. Compressive strength evolution: a) W/CM=0.557, b) W/CM=0.483, c) W/CM=0.426, d) Multi-Vari Chart

Fig. 4. Water permeability: a) W/CM=0.557, b) W/CM=0.483, c) W/CM=0.426, d) Multi-Vari Chart

Fig. 5. Chloride penetration: a) W/CM=0.557, b) W/CM=0.483, c) W/CM=0.426, d) Multi-Vari Chart

Fig. 6. Chloride diffusion coefficient: a) W/CM=0.557, b) W/CM=0.483, c) W/CM=0.426, d) Multi-Vari Chart

Fig. 7. Carbonation: a) Carbonation depth, b) Multi-Vari Chart

Fig. 8. Parameters influencing durability a) Water permeability, b) Chloride penetration, c) Chloride diffusion coefficient

**Table captions**

Table 1. Chemical and physical properties of TP fly ash

Table 2. Mineralogical composition of TP fly ash as determined by quantitative X-ray diffraction

Table 3. Mineralogical composition of cement as determined by quantitative X-ray diffraction

Table 4. Mix proportions

Table 5. Mix ID encoding (order, description and code per variable)

Table 6. Concrete tests

Fig. 1

Fig. 2



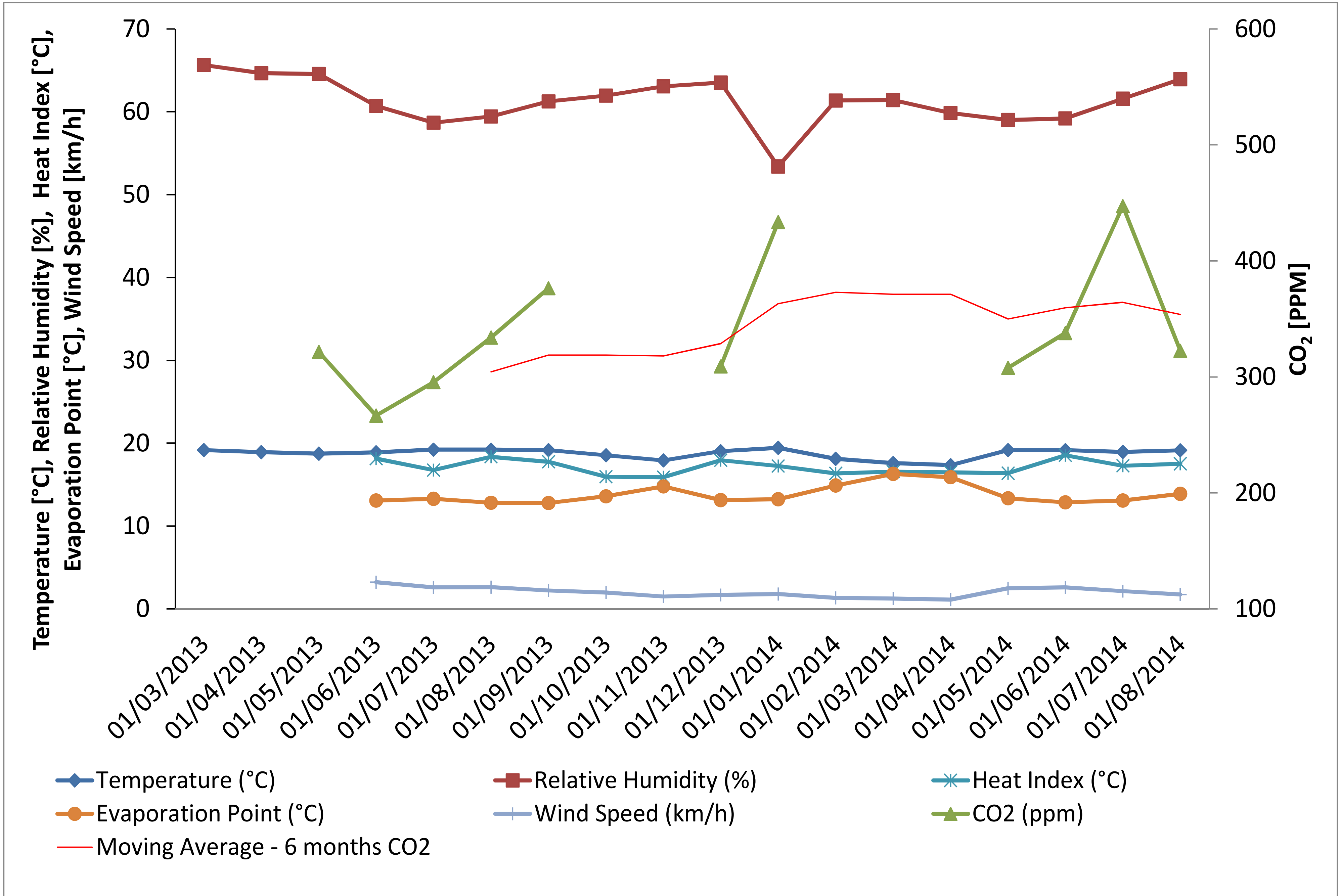
Temperature [°C], Relative Humidity [%], Heat Index [°C], Evaporation Point [°C], Wind Speed [km/h]
$CO_2$ [PPM]
70
60
50
40
30
20
10
0
600
500
400
300
200
100
01/03/2013
01/04/2013
01/05/2013
01/06/2013
01/07/2013
01/08/2013
01/09/2013
01/10/2013
01/11/2013
01/12/2013
01/01/2014
01/02/2014
01/03/2014
01/04/2014
01/05/2014
01/06/2014
01/07/2014
01/08/2014
Temperature (°C)
Relative Humidity (%)
Heat Index (°C)
Evaporation Point (°C)
Wind Speed (km/h)
CO2 (ppm)
Moving Average - 6 months CO2

Fig.3



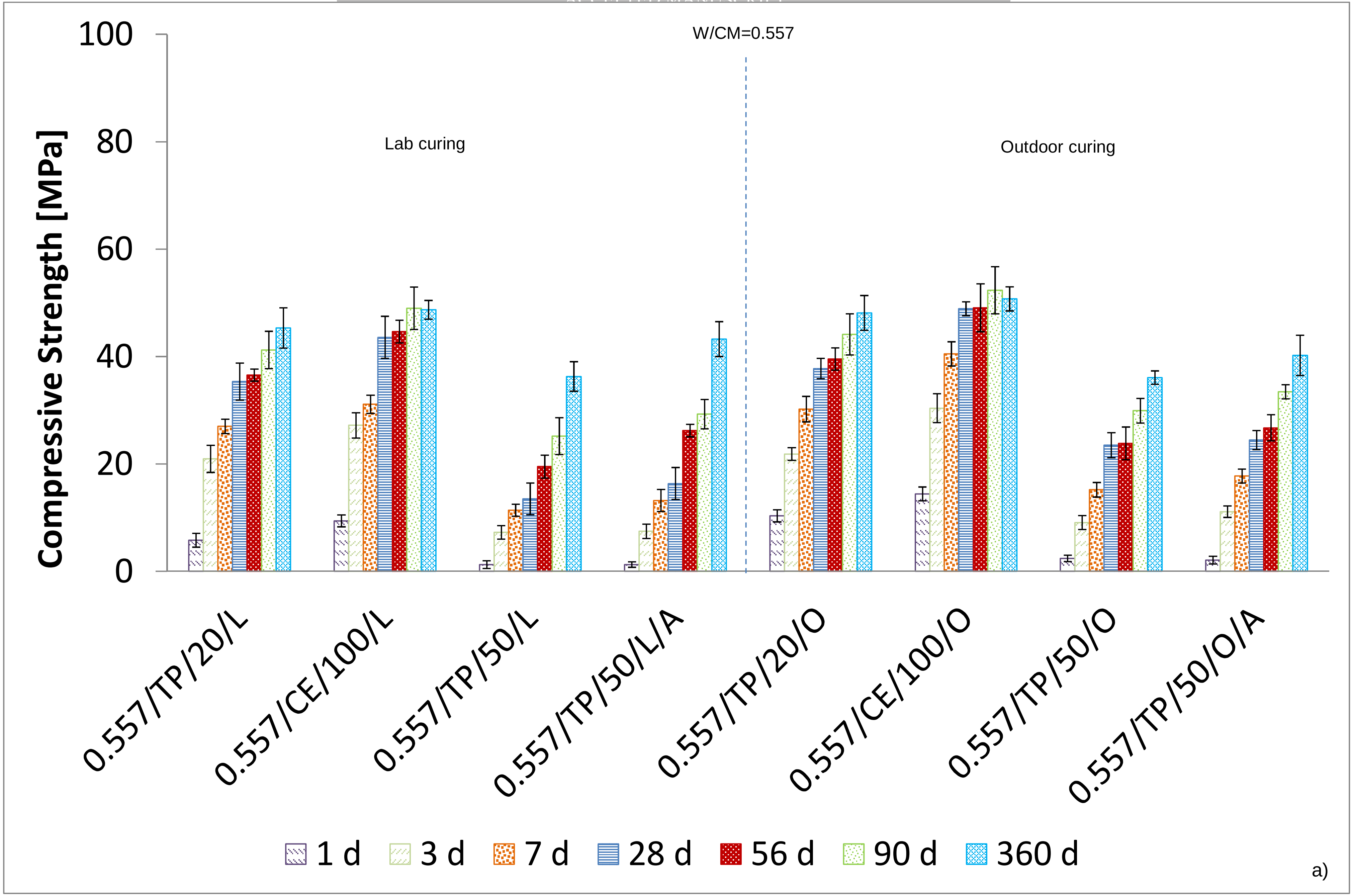
W/CM=0.557
Lab curing
Outdoor curing
Compressive Strength [MPa]
100
80
60
40
20
0
0.557/TP/20/L
0.557/CE/100/L
0.557/TP/50/L
0.557/TP/50/L/A
0.557/TP/20/O
0.557/CE/100/O
0.557/TP/50/O
0.557/TP/50/O/A
1 d
3 d
7 d
28 d
56 d
90 d
360 d
a)

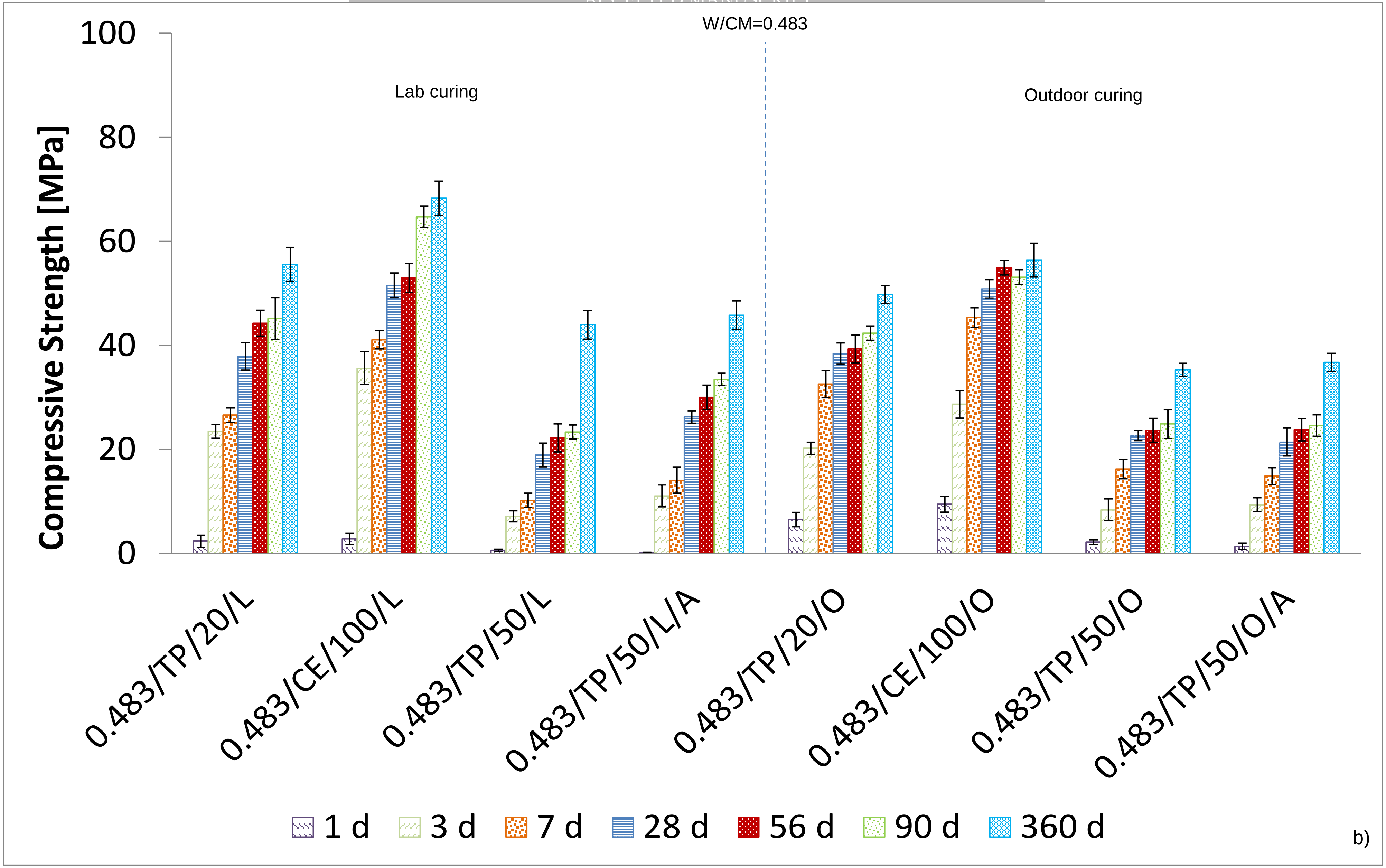
W/CM=0.483
Lab curing
Outdoor curing
Compressive Strength [MPa]
100
80
60
40
20
0
0.483/TP/20/L
0.483/CE/100/L
0.483/TP/50/L
0.483/TP/50/L/A
0.483/TP/20/O
0.483/CE/100/O
0.483/TP/50/O
0.483/TP/50/O/A
1 d
3 d
7 d
28 d
56 d
90 d
360 d
b)

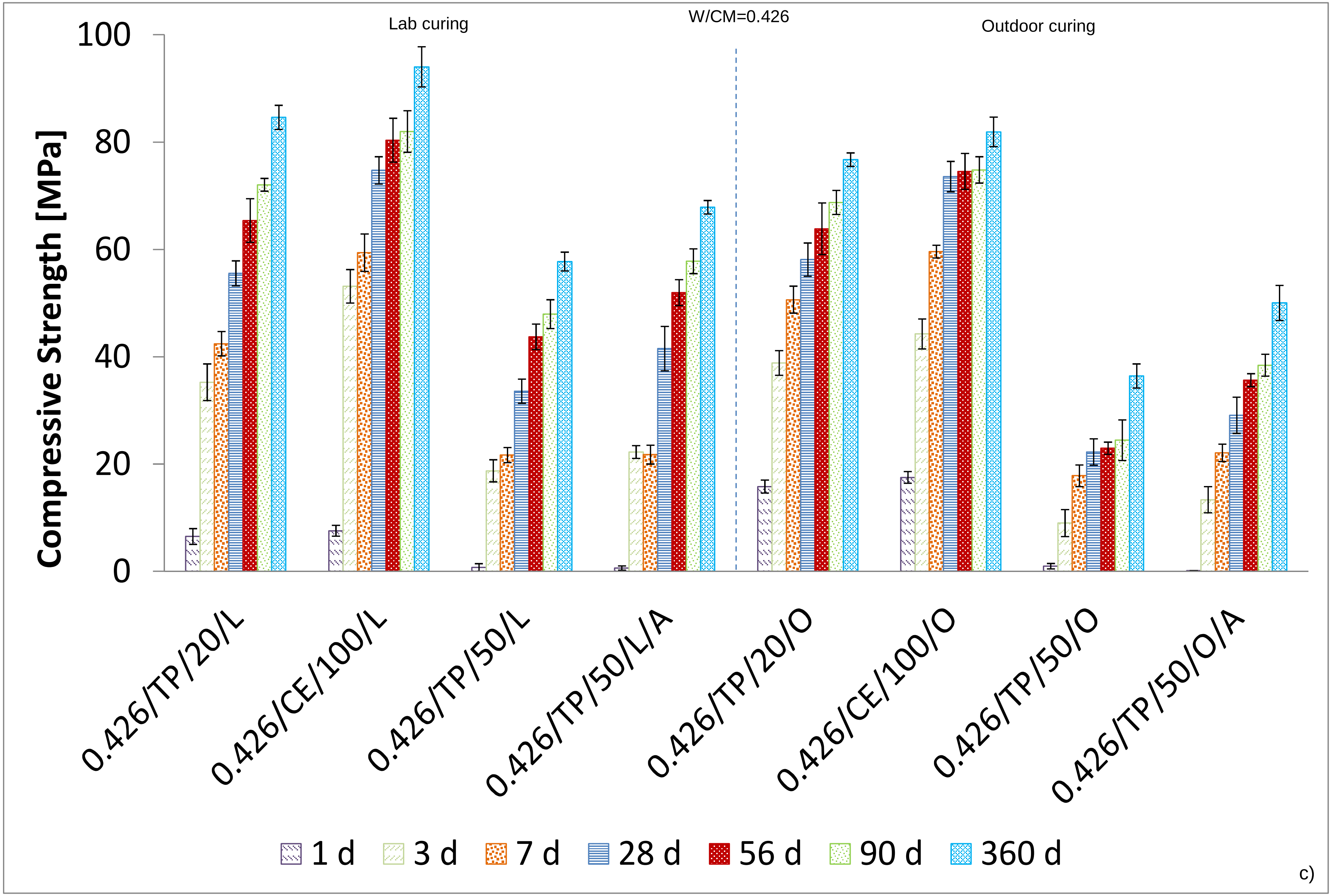

Lab curing
W/CM=0.426
Outdoor curing
Compressive Strength [MPa]
100
80
60
40
20
0
0.426/TP/20/L
0.426/CE/100/L
0.426/TP/50/L
0.426/TP/50/L/A
0.426/TP/20/O
0.426/CE/100/O
0.426/TP/50/O
0.426/TP/50/O/A
1 d
3 d
7 d
28 d
56 d
90 d
360 d
c)

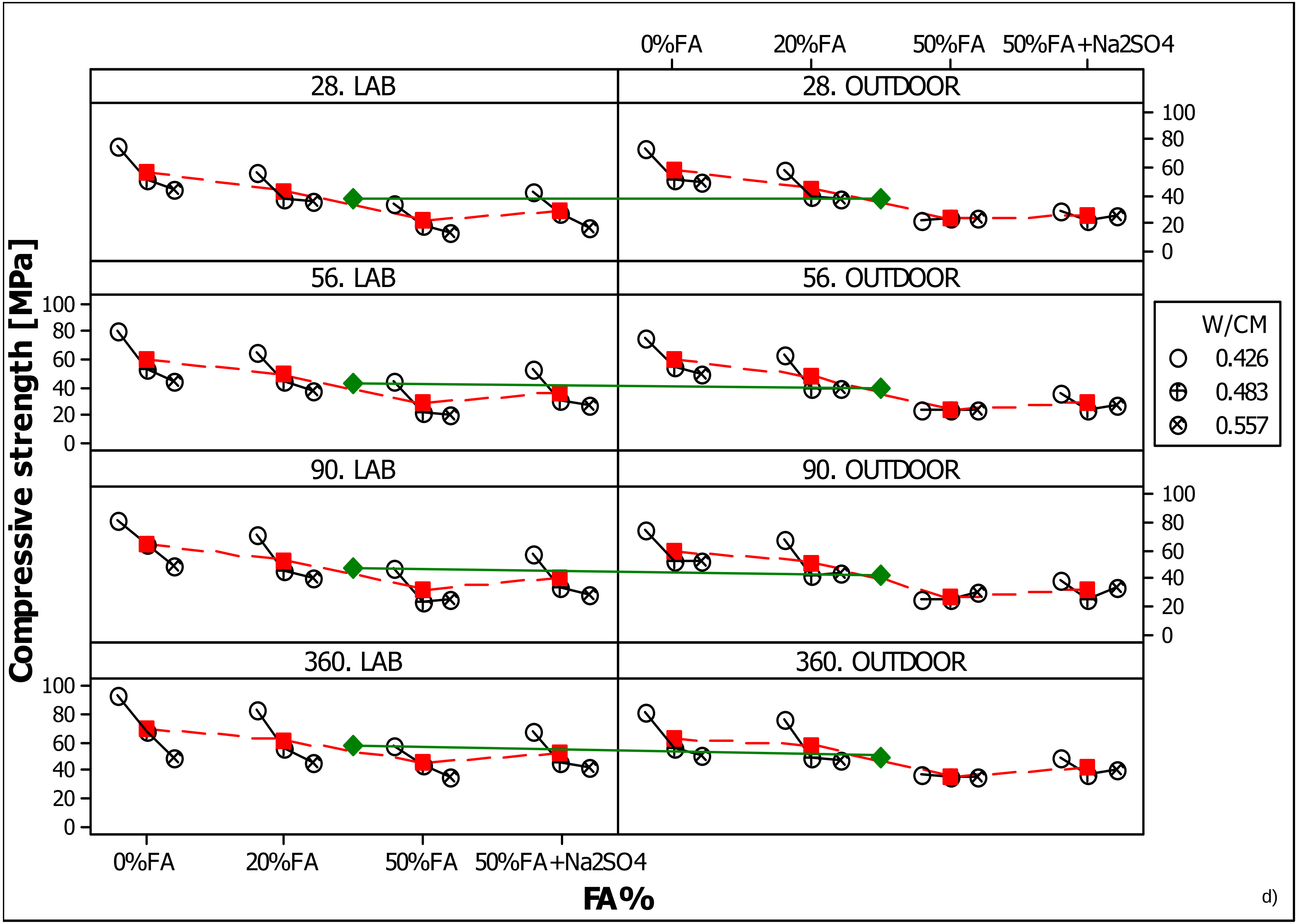
0%FA
20%FA
50%FA
50%FA+Na2SO4
28. LAB
28. OUTDOOR
56. LAB
56. OUTDOOR
90. LAB
90. OUTDOOR
360. LAB
360. OUTDOOR
100
80
60
40
20
0
W/CM
0.426
0.483
0.557
Compressive strength [MPa]
FA%
d)

Fig. 4



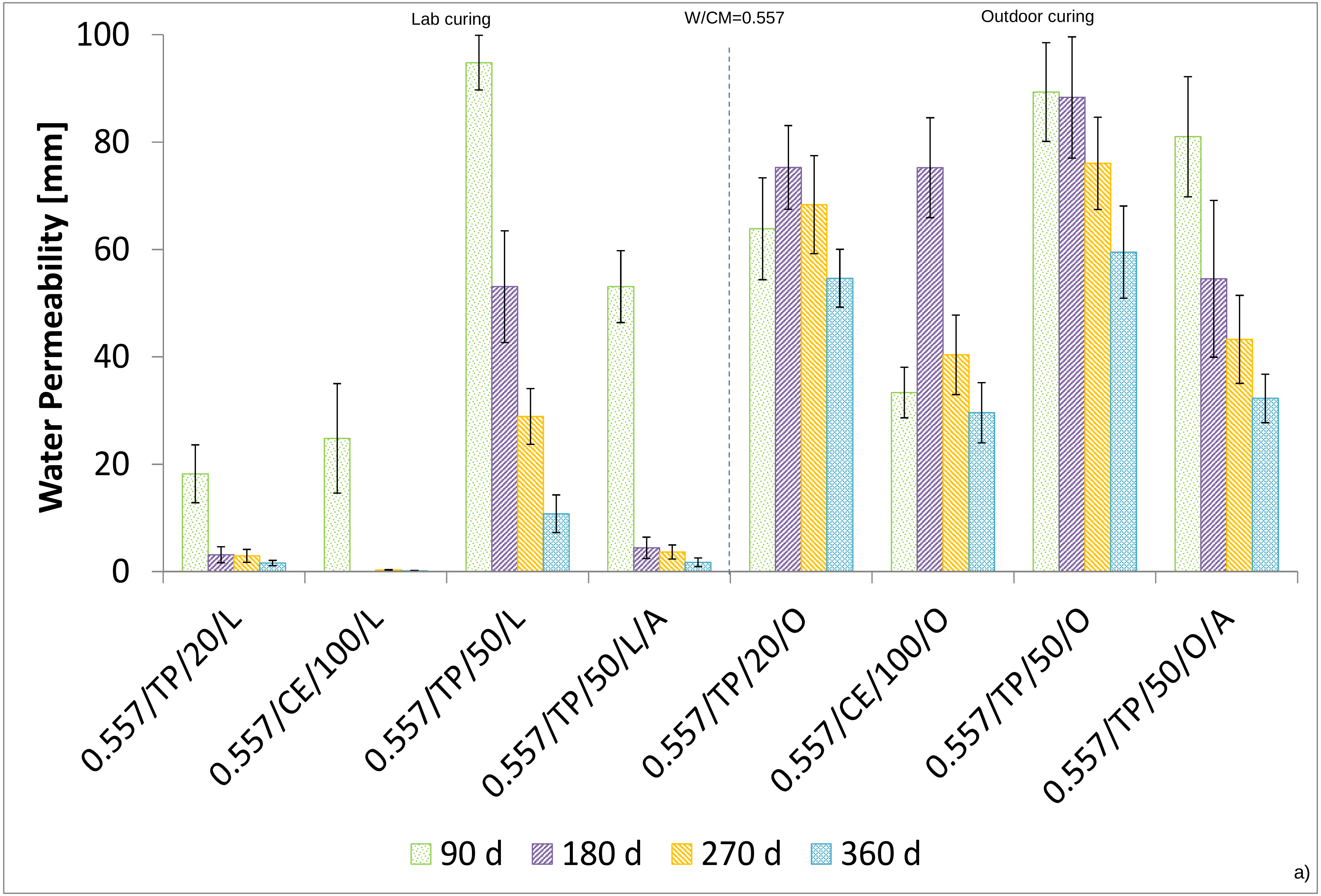
Lab curing
W/CM=0.557
Outdoor curing
Water Permeability [mm]
100
80
60
40
20
0
0.557/TP/20/L
0.557/CE/100/L
0.557/TP/50/L
0.557/TP/50/L/A
0.557/TP/20/O
0.557/CE/100/O
0.557/TP/50/O
0.557/TP/50/O/A
90 d
180 d
270 d
360 d
a)

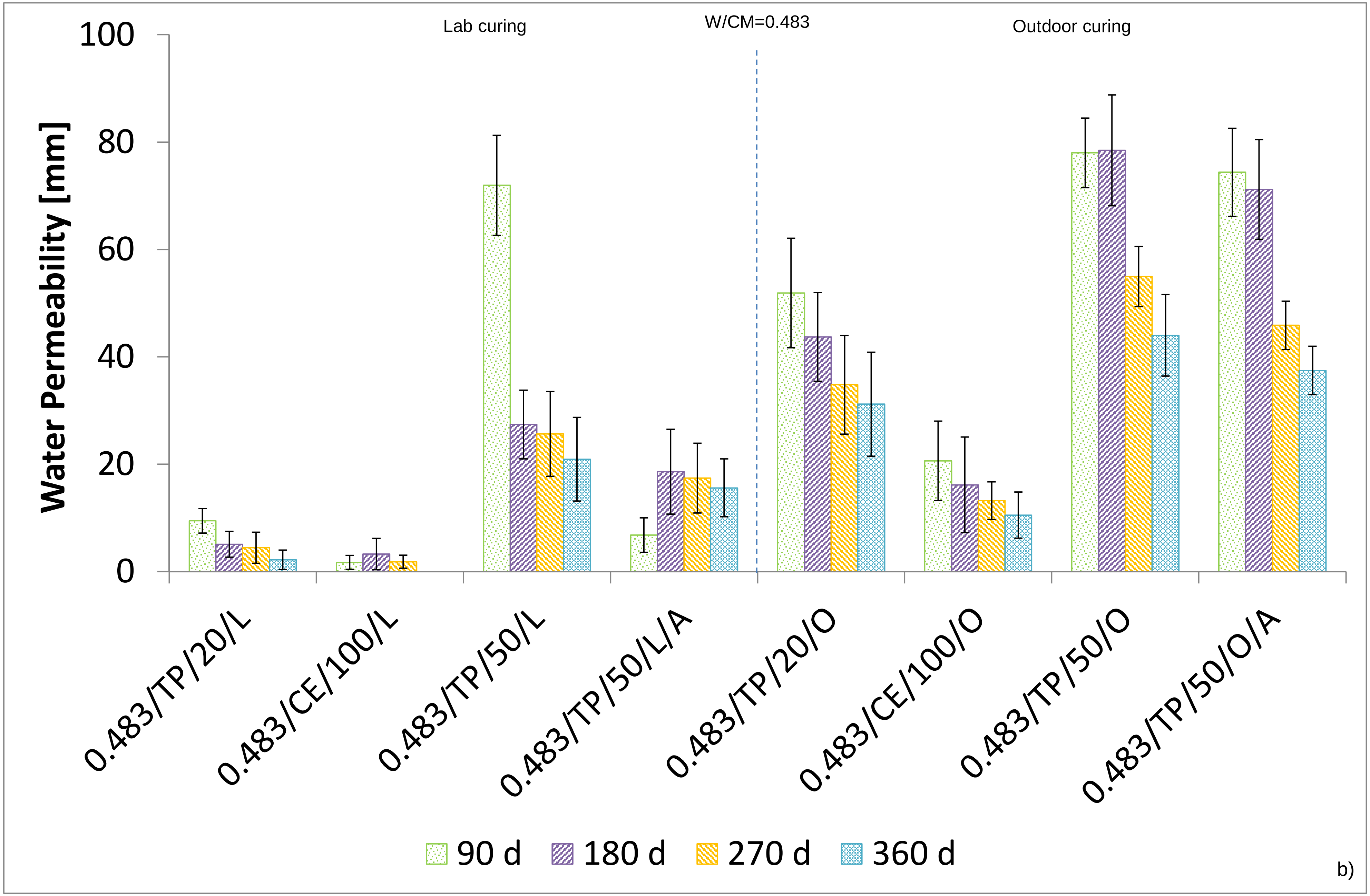
Lab curing
W/CM=0.483
Outdoor curing
100
80
60
40
20
0
Water Permeability [mm]
0.483/TP/20/L
0.483/CE/100/L
0.483/TP/50/L
0.483/TP/50/L/A
0.483/TP/20/O
0.483/CE/100/O
0.483/TP/50/O
0.483/TP/50/O/A
90 d
180 d
270 d
360 d
b)

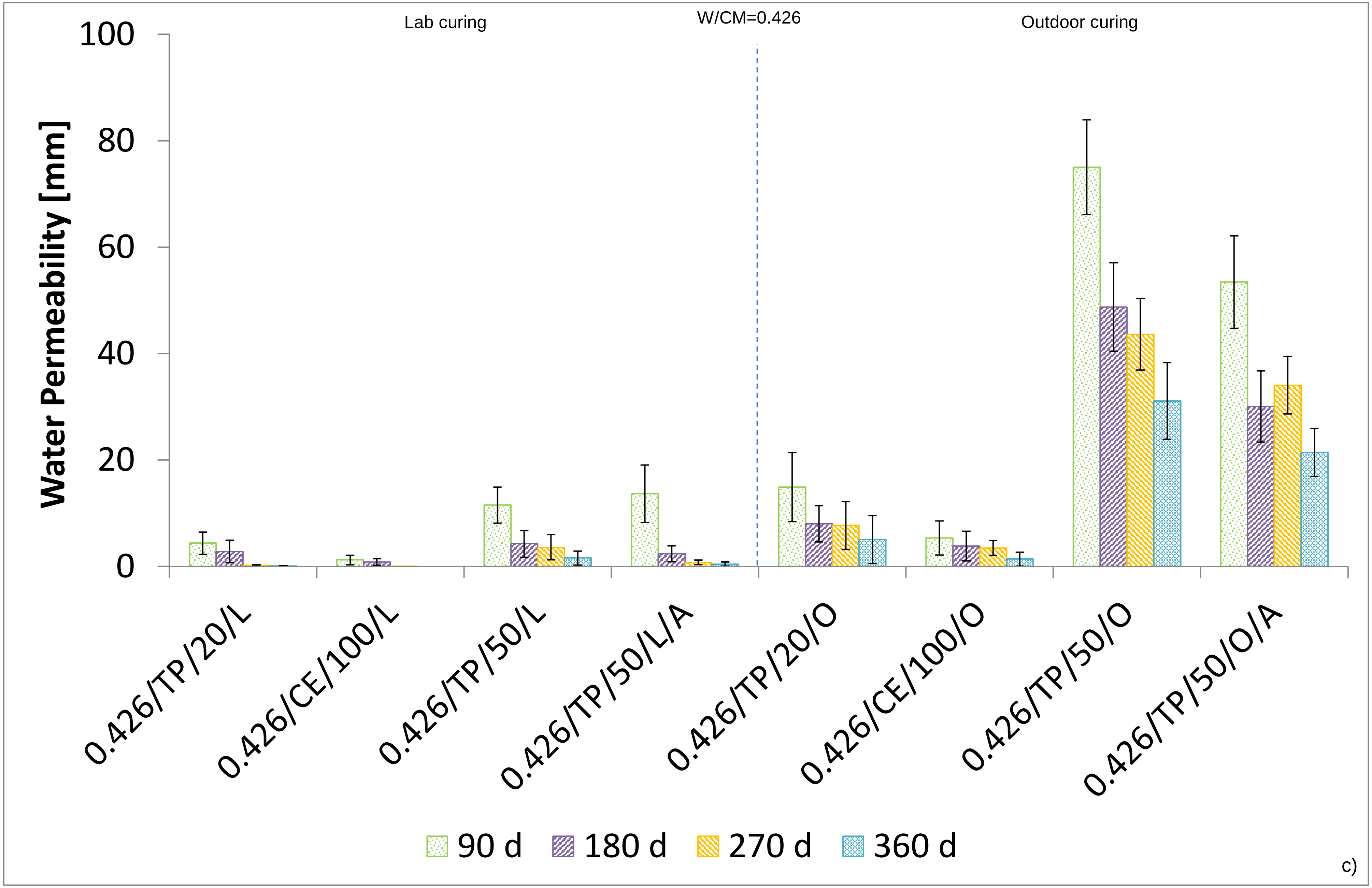
Lab curing
W/CM=0.426
Outdoor curing
Water Permeability [mm]
100
80
60
40
20
0
0.426/TP/20/L
0.426/CE/100/L
0.426/TP/50/L
0.426/TP/50/L/A
0.426/TP/20/O
0.426/CE/100/O
0.426/TP/50/O
0.426/TP/50/O/A
90 d
180 d
270 d
360 d
c)

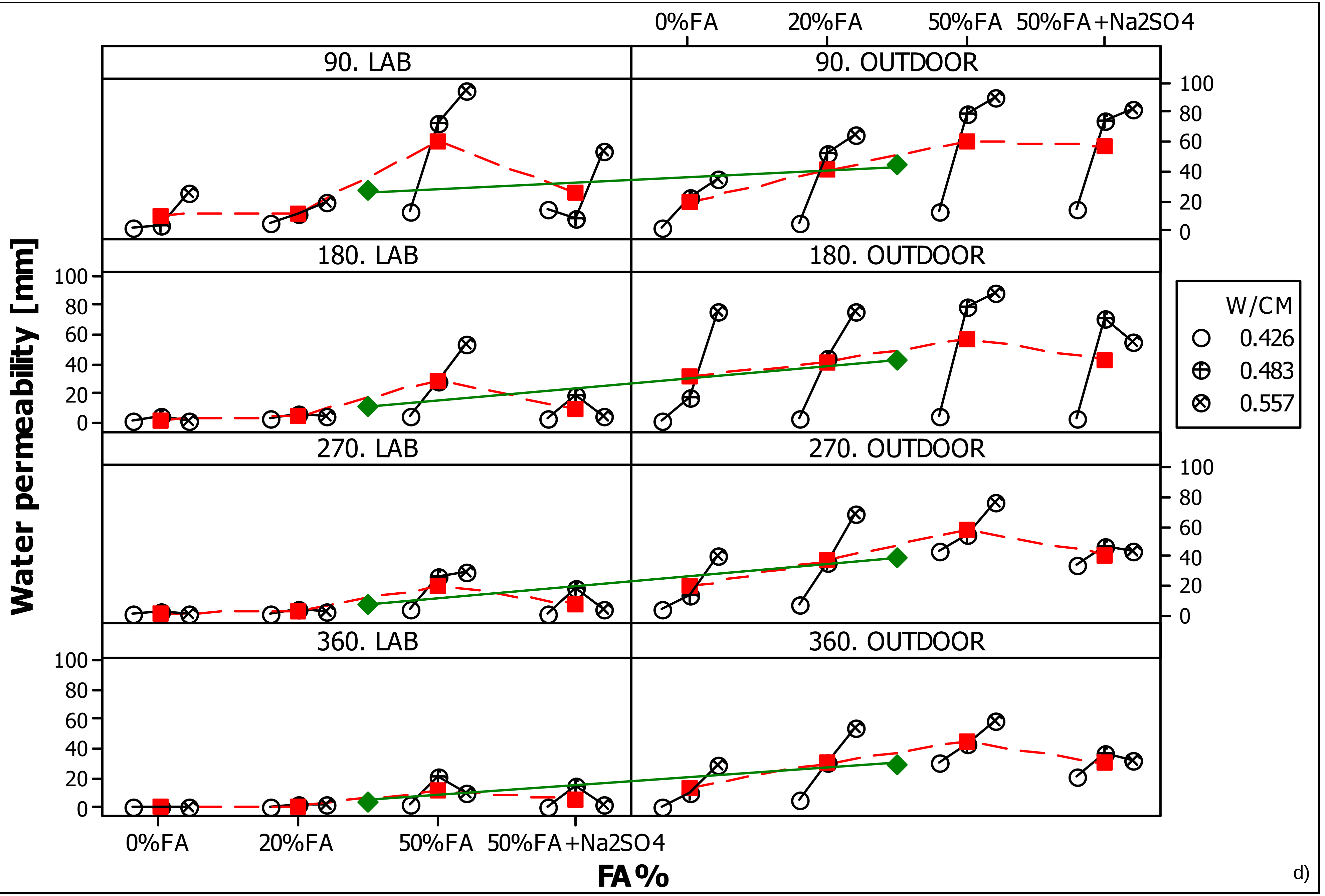

0%FA
20%FA
50%FA
50%FA+Na2SO4
90. LAB
90. OUTDOOR
180. LAB
180. OUTDOOR
270. LAB
270. OUTDOOR
360. LAB
360. OUTDOOR
100
80
60
40
20
0
W/CM
0.426
0.483
0.557
Water permeability [mm]
FA%


d)

Fig. 5



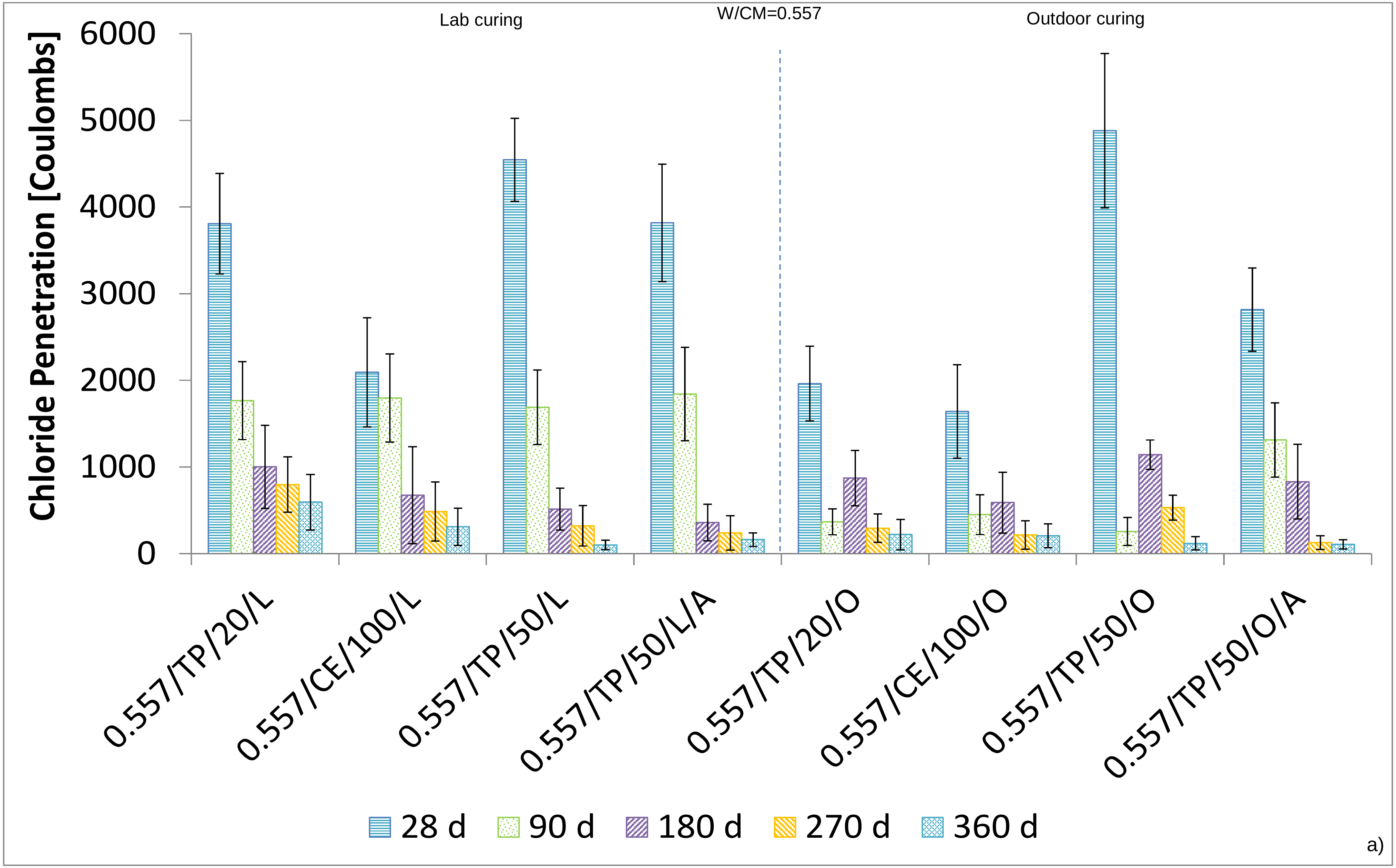
Lab curing
W/CM=0.557
Outdoor curing
Chloride Penetration [Coulombs]
6000
5000
4000
3000
2000
1000
0
0.557/TP/20/L
0.557/CE/100/L
0.557/TP/50/L
0.557/TP/50/L/A
0.557/TP/20/O
0.557/CE/100/O
0.557/TP/50/O
0.557/TP/50/O/A
28 d
90 d
180 d
270 d
360 d
a)

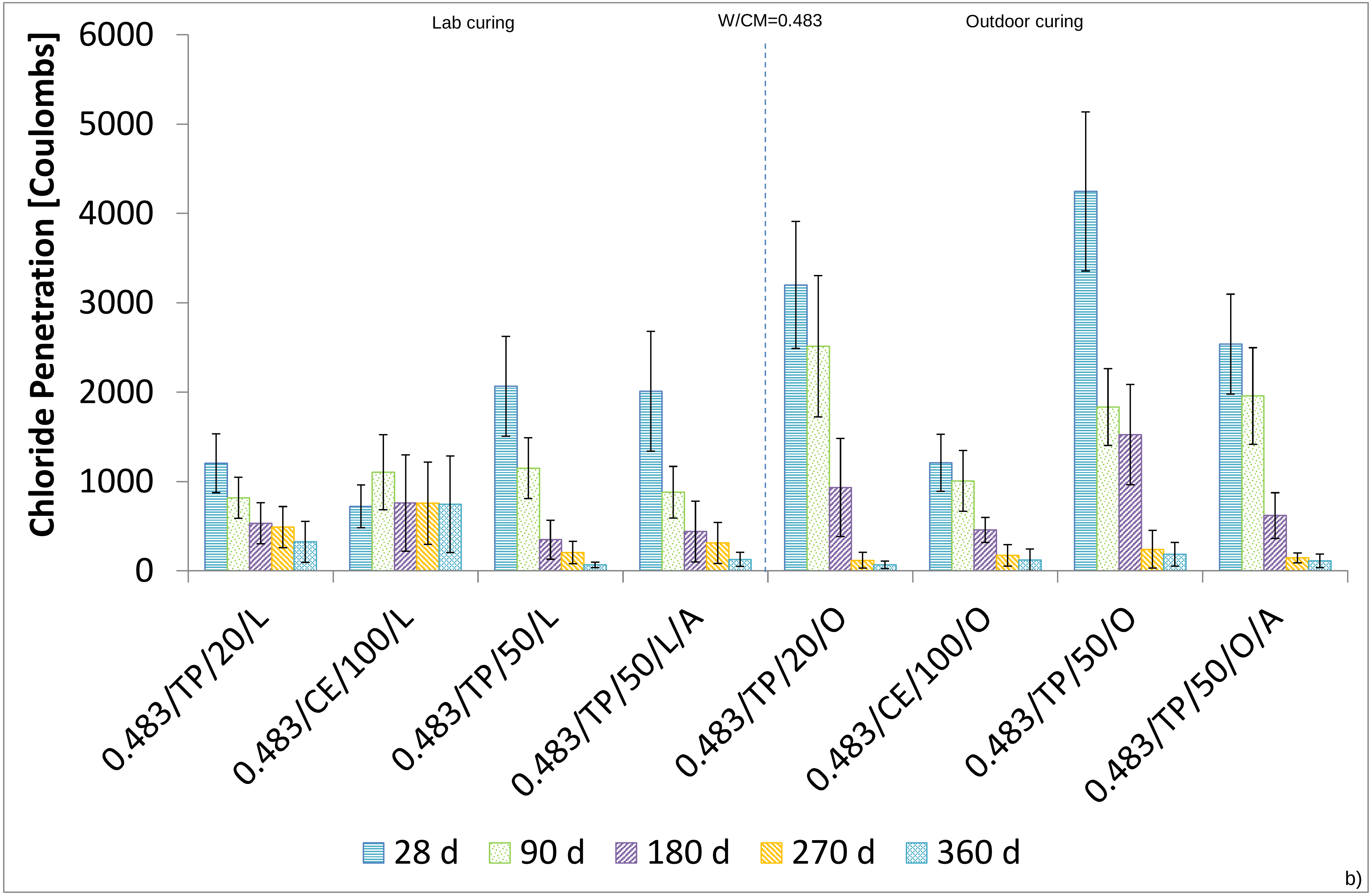
Chloride Penetration [Coulombs]
0
1000
2000
3000
4000
5000
6000
Lab curing
W/CM=0.483
Outdoor curing
0.483/TP/20/L
0.483/CE/100/L
0.483/TP/50/L
0.483/TP/50/L/A
0.483/TP/20/O
0.483/CE/100/O
0.483/TP/50/O
0.483/TP/50/O/A
28 d
90 d
180 d
270 d
360 d
b)

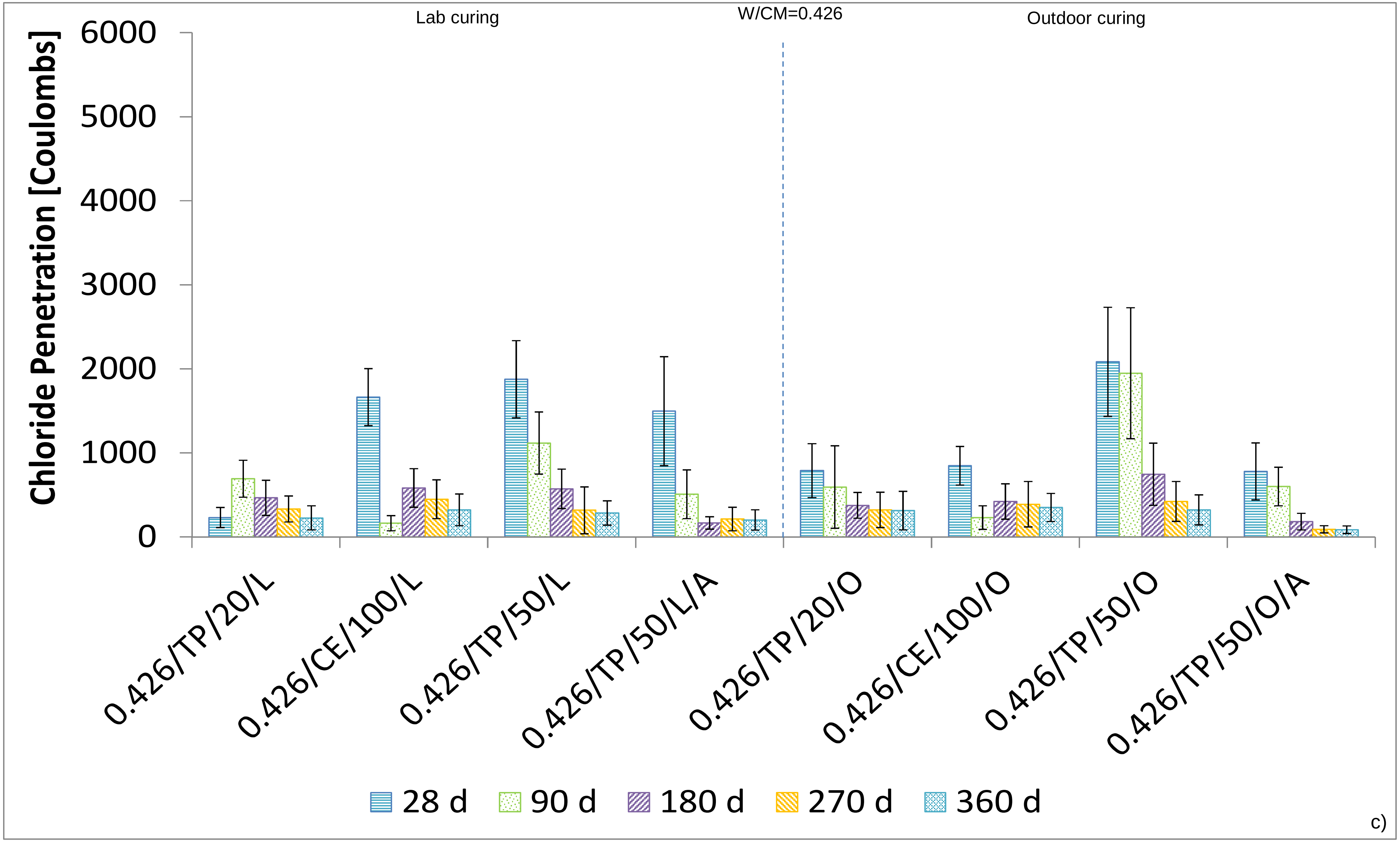

Lab curing
W/CM=0.426
Outdoor curing
Chloride Penetration [Coulombs]
6000
5000
4000
3000
2000
1000
0
0.426/TP/20/L
0.426/CE/100/L
0.426/TP/50/L
0.426/TP/50/L/A
0.426/TP/20/O
0.426/CE/100/O
0.426/TP/50/O
0.426/TP/50/O/A
28 d
90 d
180 d
270 d
360 d
c)

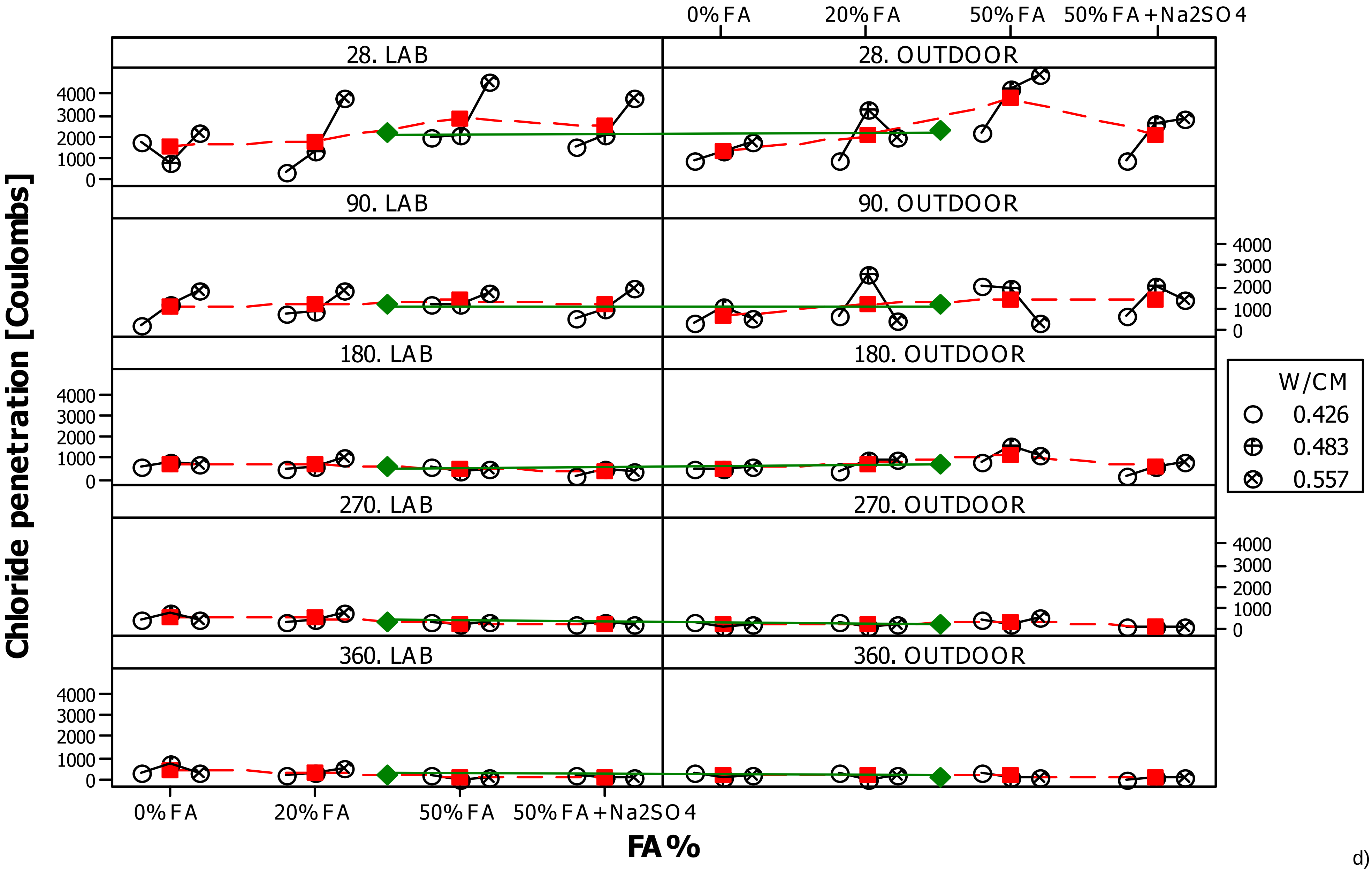

0% FA
20% FA
50% FA
50% FA+Na2SO4
28. LAB
28. OUTDOOR
90. LAB
90. OUTDOOR
180. LAB
180. OUTDOOR
270. LAB
270. OUTDOOR
360. LAB
360. OUTDOOR
4000
3000
2000
1000
0
W/CM
0.426
0.483
0.557
Chloride penetration [Coulombs]
FA%


d)

Fig. 6



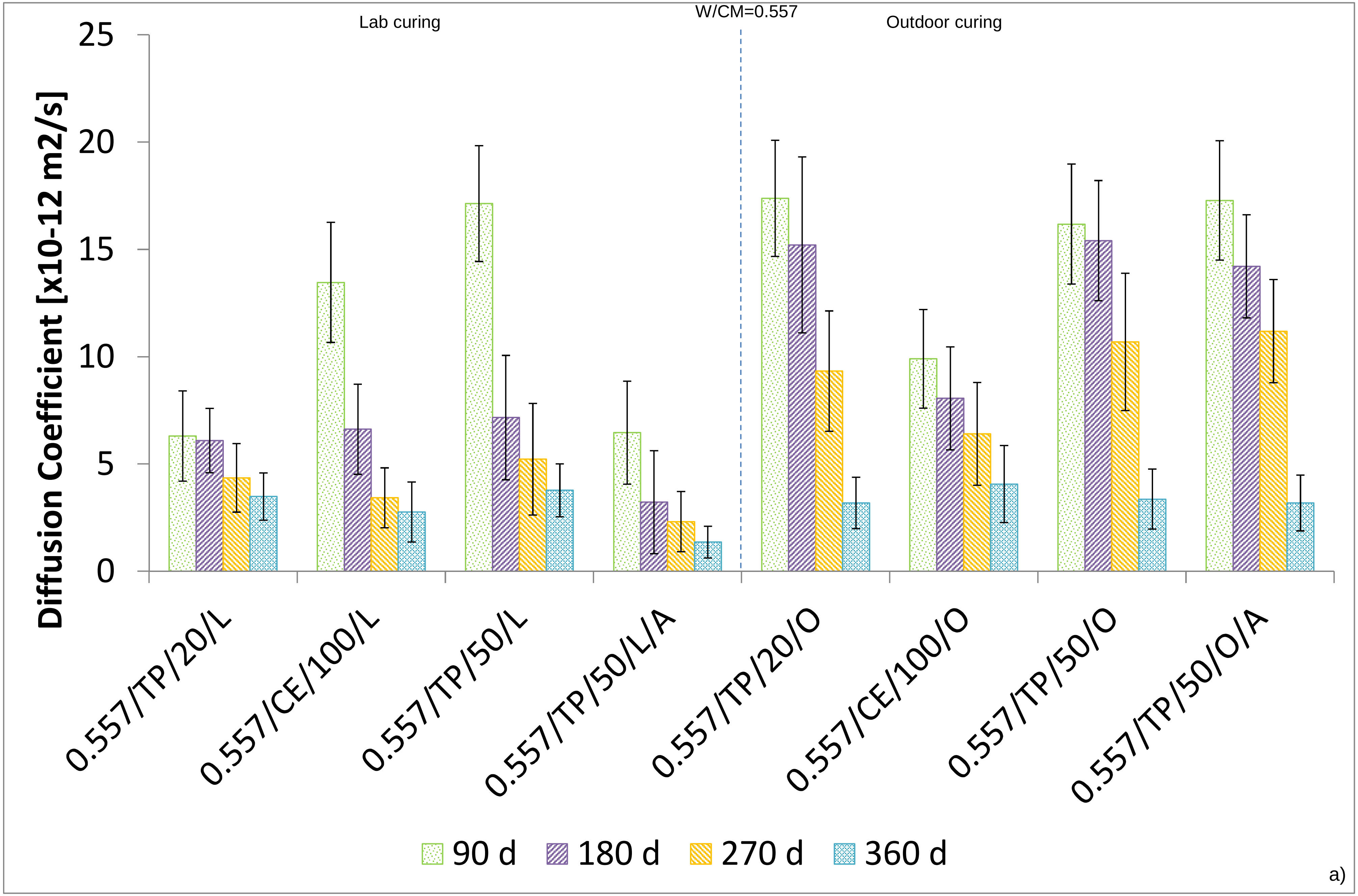
W/CM=0.557
Lab curing
Outdoor curing
Diffusion Coefficient [x10-12 m2/s]
25
20
15
10
5
0
0.557/TP/20/L
0.557/CE/100/L
0.557/TP/50/L
0.557/TP/50/L/A
0.557/TP/20/O
0.557/CE/100/O
0.557/TP/50/O
0.557/TP/50/O/A
90 d
180 d
270 d
360 d
a)

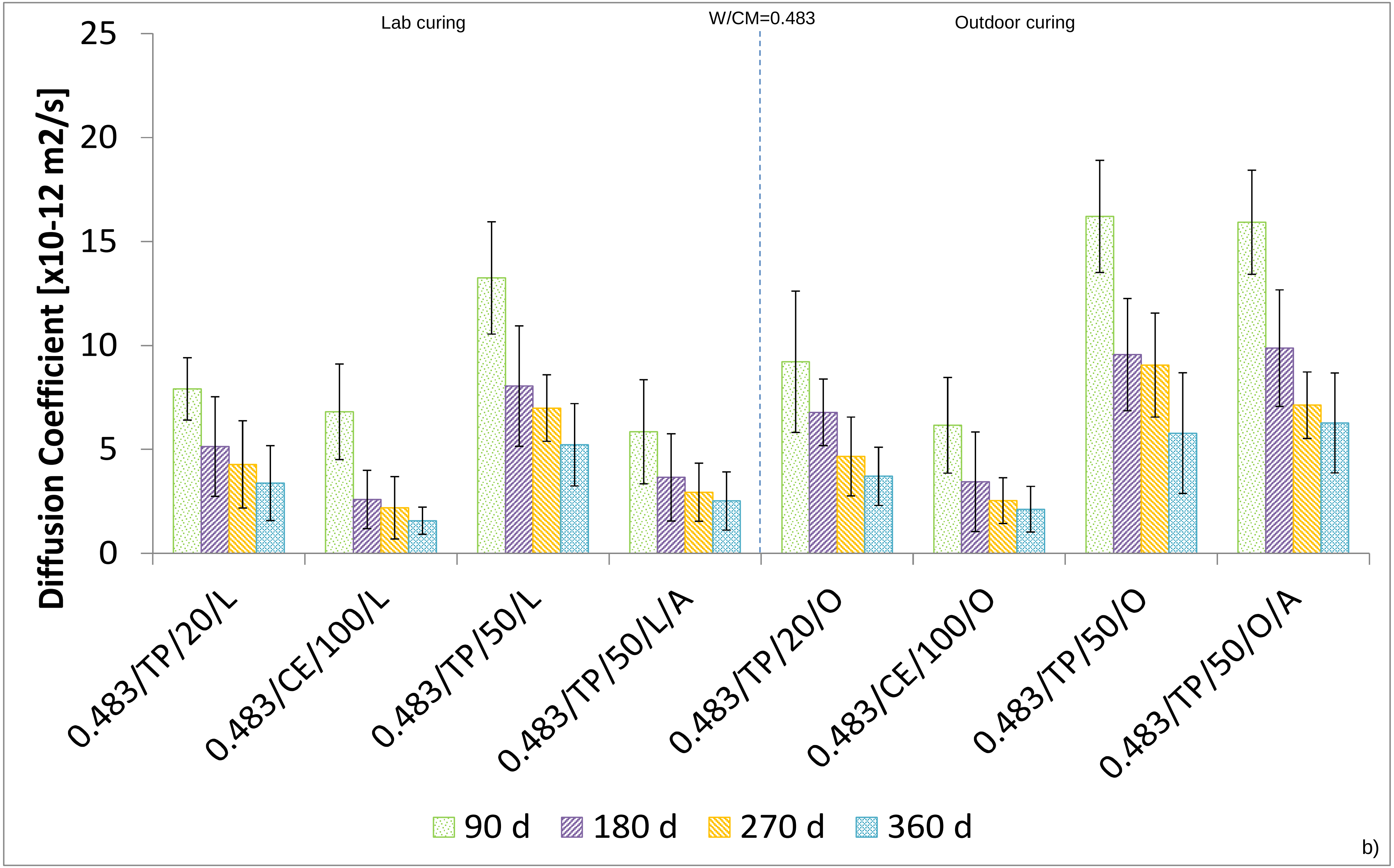

Lab curing
W/CM=0.483
Outdoor curing
Diffusion Coefficient [x10-12 m2/s]
25
20
15
10
5
0
0.483/TP/20/L
0.483/CE/100/L
0.483/TP/50/L
0.483/TP/50/L/A
0.483/TP/20/O
0.483/CE/100/O
0.483/TP/50/O
0.483/TP/50/O/A
90 d
180 d
270 d
360 d
b)

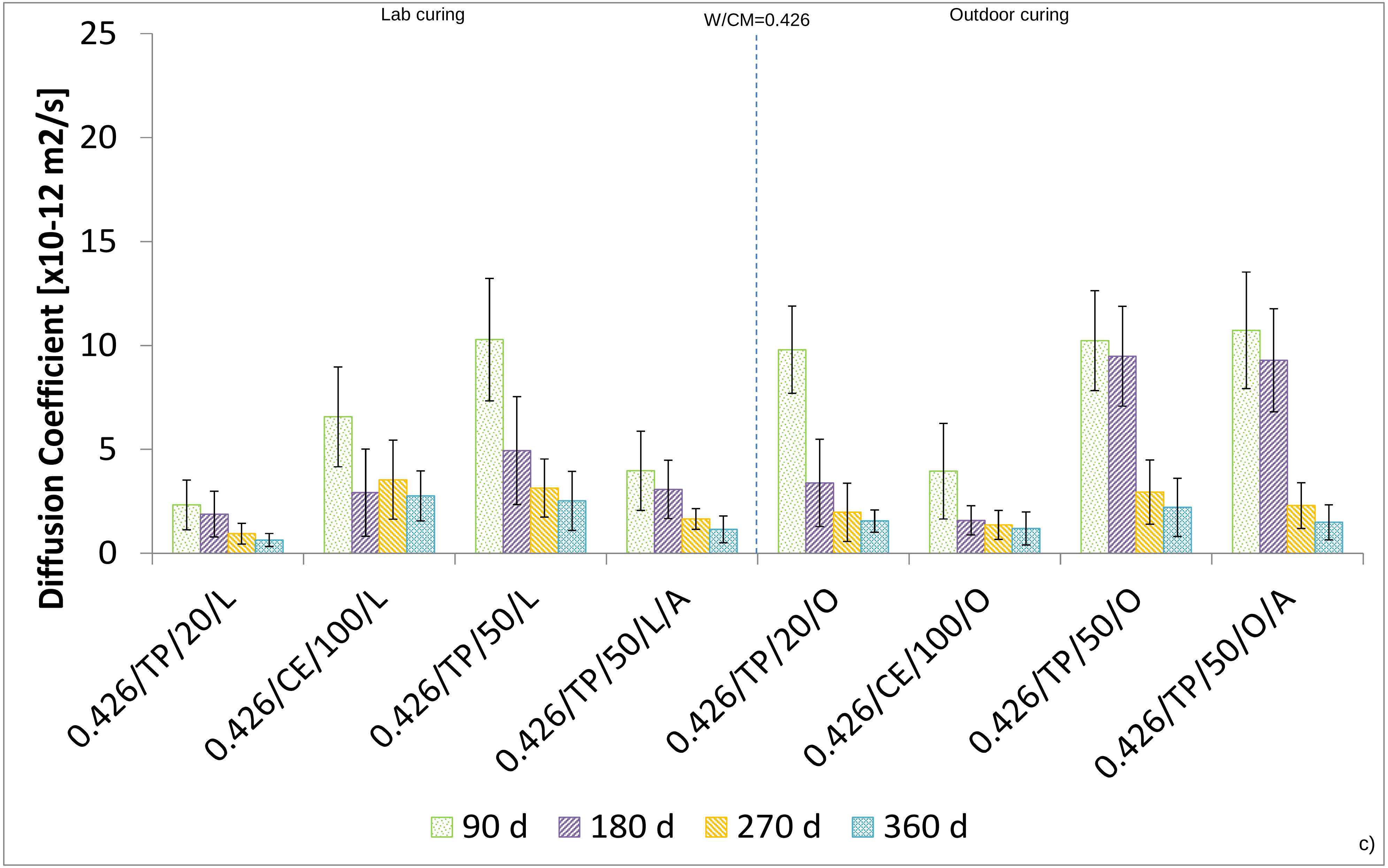
Lab curing
W/CM=0.426
Outdoor curing
Diffusion Coefficient [x10-12 m2/s]
25
20
15
10
5
0
0.426/TP/20/L
0.426/CE/100/L
0.426/TP/50/L
0.426/TP/50/L/A
0.426/TP/20/O
0.426/CE/100/O
0.426/TP/50/O
0.426/TP/50/O/A
90 d
180 d
270 d
360 d
c)

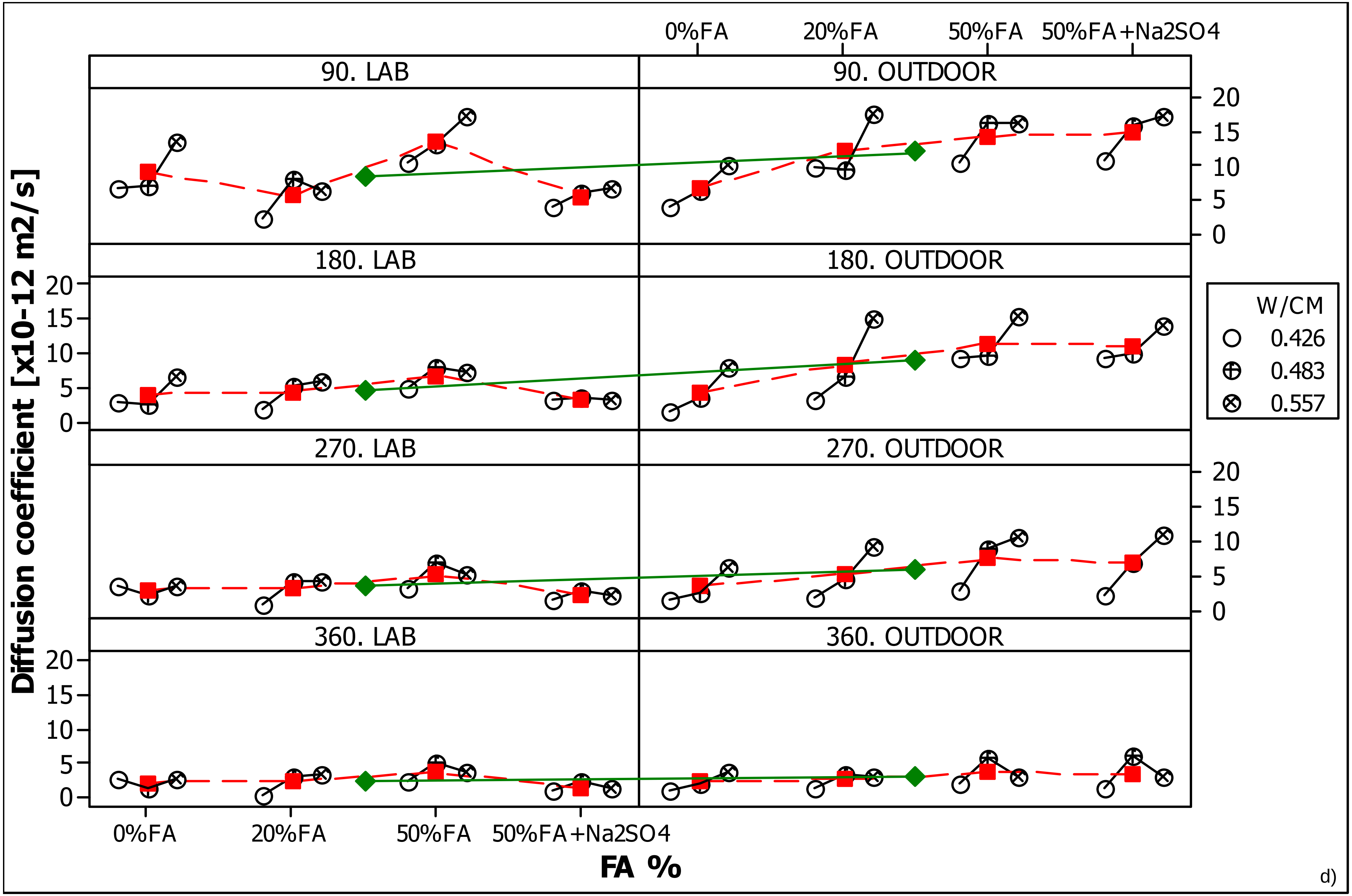
90. LAB
90. OUTDOOR
180. LAB
180. OUTDOOR
270. LAB
270. OUTDOOR
360. LAB
360. OUTDOOR
0%FA
20%FA
50%FA
50%FA+Na2SO4
0
5
10
15
20
Diffusion coefficient [x10-12 m2/s]
FA %
W/CM
0.426
0.483
0.557
d)

Fig. 7

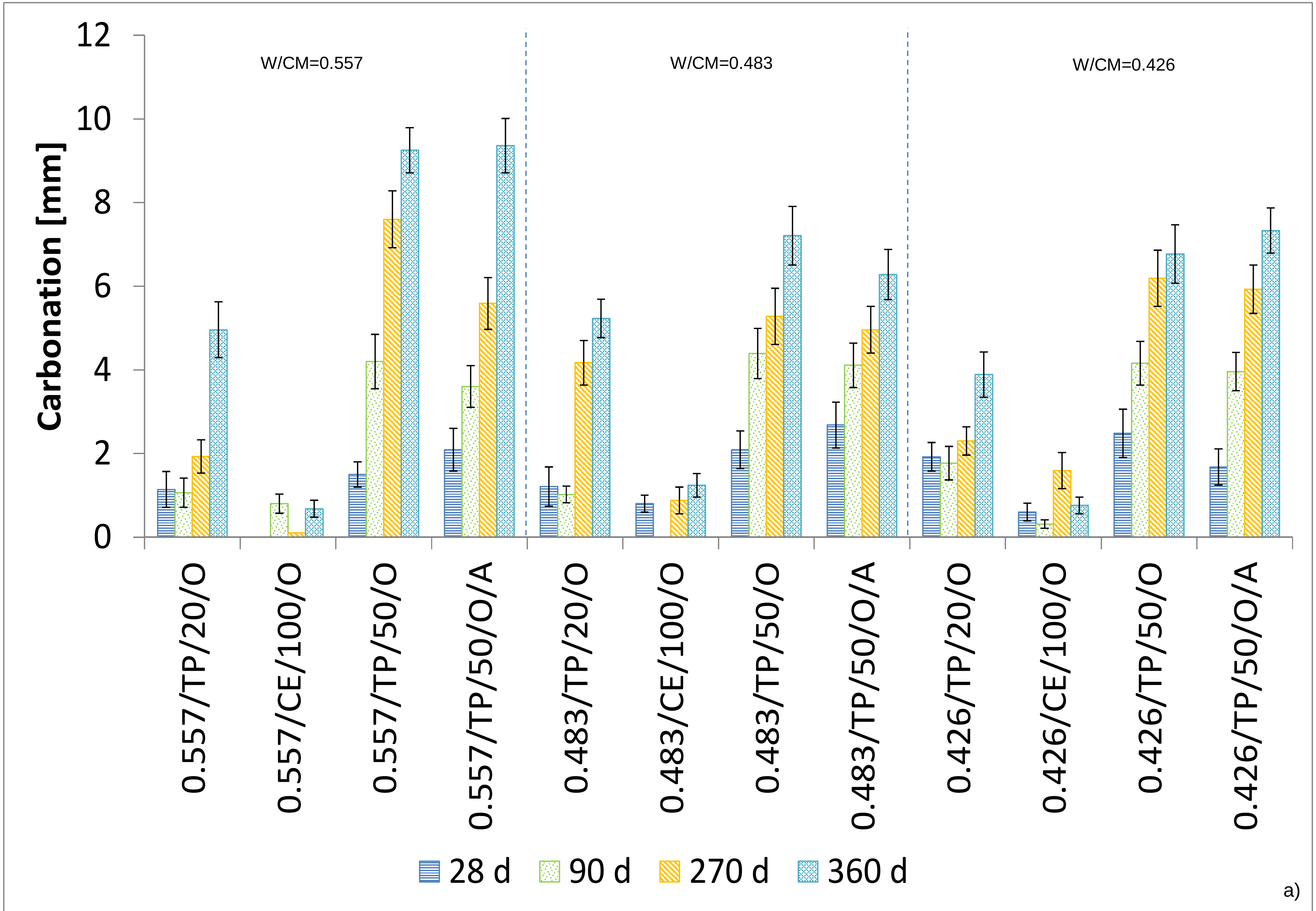

Carbonation [mm]
0
2
4
6
8
10
12
W/CM=0.557
W/CM=0.483
W/CM=0.426
0.557/TP/20/O
0.557/CE/100/O
0.557/TP/50/O
0.557/TP/50/O/A
0.483/TP/20/O
0.483/CE/100/O
0.483/TP/50/O
0.483/TP/50/O/A
0.426/TP/20/O
0.426/CE/100/O
0.426/TP/50/O
0.426/TP/50/O/A
28 d
90 d
270 d
360 d
a)

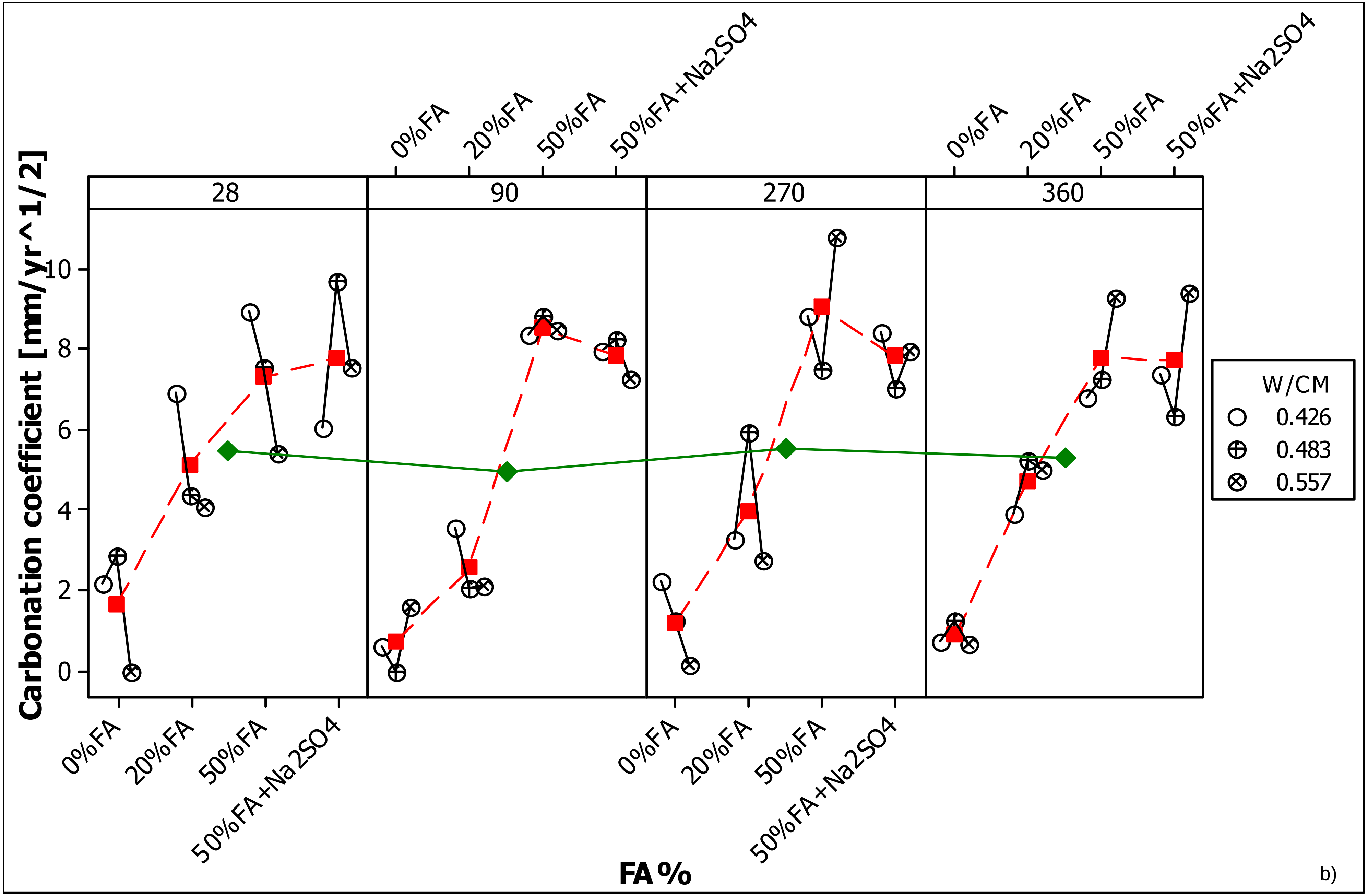

Carbonation coefficient [mm/yr^1/2]
FA %
28
90
270
360
0%FA
20%FA
50%FA
50%FA+Na2SO4
0
2
4
6
8
10
W/CM
0.426
0.483
0.557
b)

Fig. 8



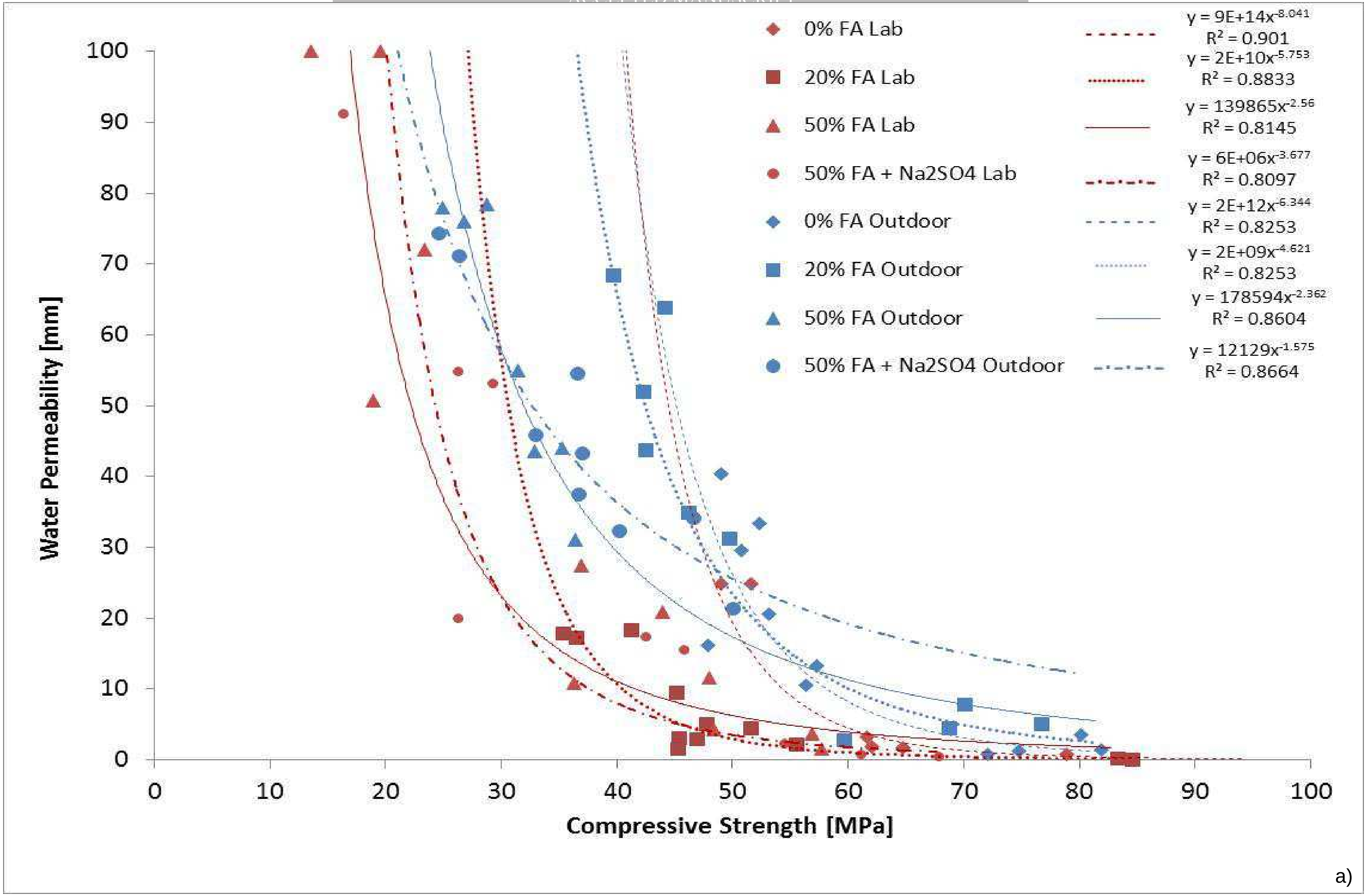
0% FA Lab
20% FA Lab
50% FA Lab
50% FA + Na2SO4 Lab
0% FA Outdoor
20% FA Outdoor
50% FA Outdoor
50% FA + Na2SO4 Outdoor
y = 9E+14x-8.041
R² = 0.901
y = 2E+10x-5.753
R² = 0.8833
y = 139865x-2.56
R² = 0.8145
y = 6E+06x-3.677
R² = 0.8097
y = 2E+12x-6.344
R² = 0.8253
y = 2E+09x-4.621
R² = 0.8253
y = 178594x-2.362
R² = 0.8604
y = 12129x-1.575
R² = 0.8664
Water Permeability [mm]
Compressive Strength [MPa]
0
10
20
30
40
50
60
70
80
90
100
a)

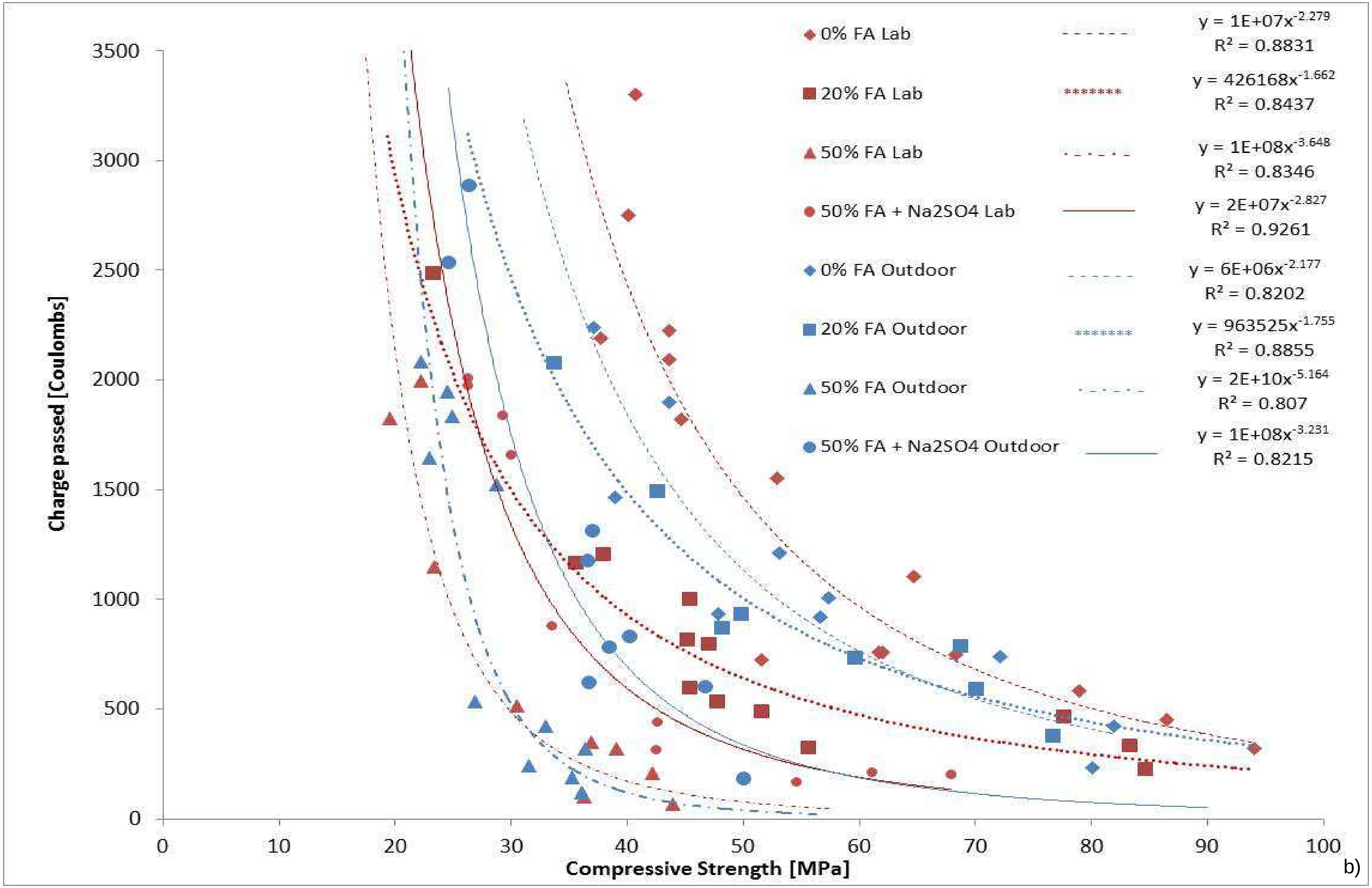

0% FA Lab
y = 1E+07x-2.279
R² = 0.8831
20% FA Lab
y = 426168x-1.662
R² = 0.8437
50% FA Lab
y = 1E+08x-3.648
R² = 0.8346
50% FA + Na2SO4 Lab
y = 2E+07x-2.827
R² = 0.9261
0% FA Outdoor
y = 6E+06x-2.177
R² = 0.8202
20% FA Outdoor
y = 963525x-1.755
R² = 0.8855
50% FA Outdoor
y = 2E+10x-5.164
R² = 0.807
50% FA + Na2SO4 Outdoor
y = 1E+08x-3.231
R² = 0.8215
Charge passed [Coulombs]
3500
3000
2500
2000
1500
1000
500
0
0
10
20
30
40
50
60
70
80
90
100
Compressive Strength [MPa]

b)

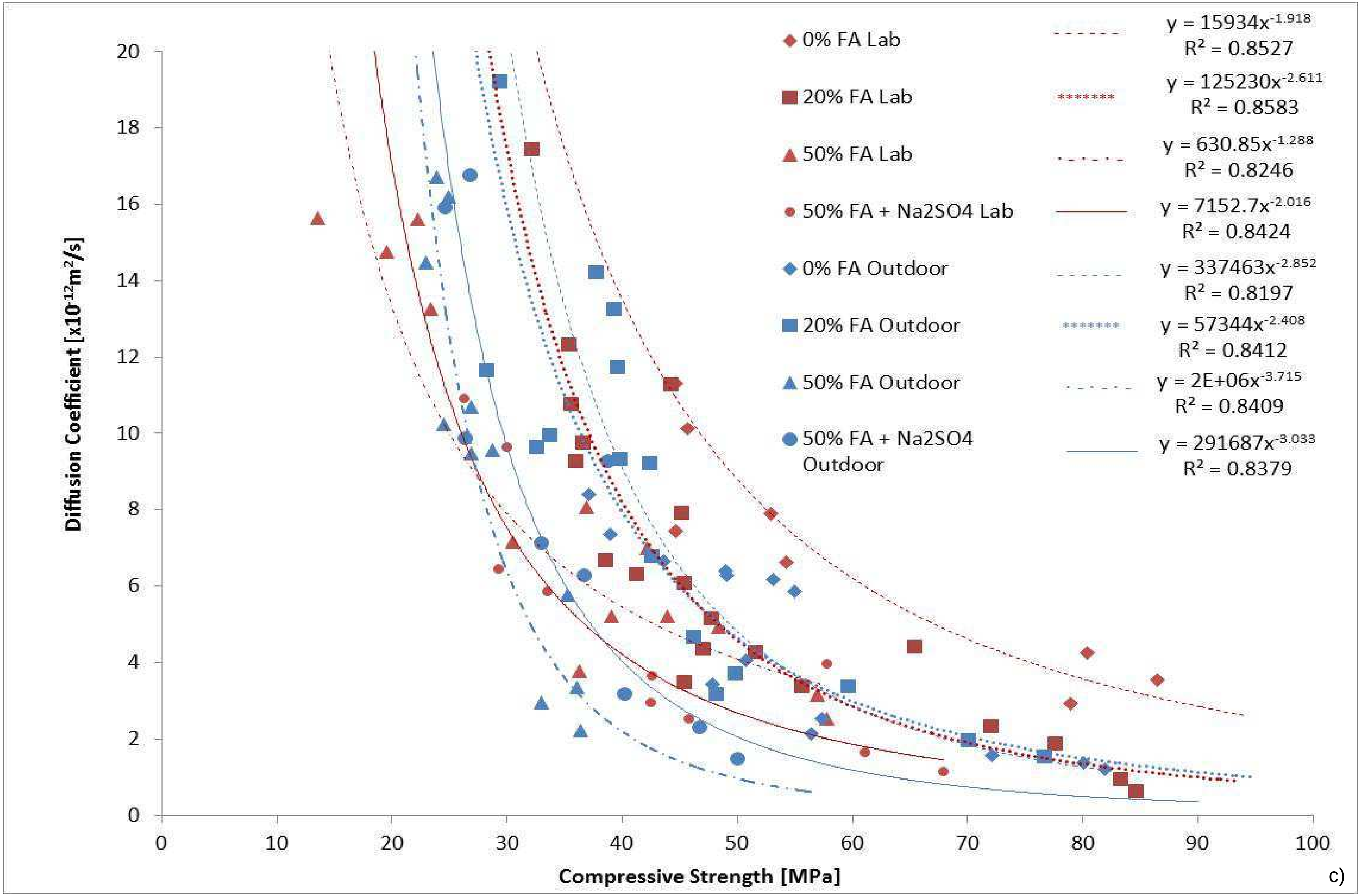

Diffusion Coefficient [x10-12m2/s]
Compressive Strength [MPa]
0% FA Lab
y = 15934x-1.918
R² = 0.8527
20% FA Lab
y = 125230x-2.611
R² = 0.8583
50% FA Lab
y = 630.85x-1.288
R² = 0.8246
50% FA + Na2SO4 Lab
y = 7152.7x-2.016
R² = 0.8424
0% FA Outdoor
y = 337463x-2.852
R² = 0.8197
20% FA Outdoor
y = 57344x-2.408
R² = 0.8412
50% FA Outdoor
y = 2E+06x-3.715
R² = 0.8409
50% FA + Na2SO4 Outdoor
y = 291687x-3.033
R² = 0.8379
0 2 4 6 8 10 12 14 16 18 20
0 10 20 30 40 50 60 70 80 90 100
c)

Table 1



| Chemical and physical properties of the fly ash | | | | | | | | | | | |
|---|---|---|---|---|---|---|---|---|---|---|---|
| **$SiO_2$ (%)** | **$Al_2O_3$ (%)** | **$Fe_2O_3$ (%)** | **$(SiO_2)+(Al_2O_3)+(Fe_2O_3)$ (%)** | **$SO_3$ (%)** | **$Na_2O$ (%)** | **CaO (%)** | **$K_2O$ (%)** | **MgO (%)** | **LOI (%)** | **Density ($g/cm^3$)** | **Retained on # 325 sieve (%)** |
| 56.67 | 20.65 | 4.92 | 82.24 | 0.06 | 0.07 | 3.27 | 1.59 | 0.62 | 10.74 | 2.09 | 38.2 |

Table 2



| Mineralogical Composition of Fly ash (%) | | | | |
|---|---|---|---|---|
| **Quartz** | **Mullite** | **Hematite** | **Calcite** | **Amorphous material** |
| 18 | 15.1 | 0.7 | 1.2 | 64.5 |

Table 3



| Mineralogical Composition of Cement (%) | | | | | |
|---|---|---|---|---|---|
| **$C_3S$** | **$C_2S$** | **$C_4AF$** | **$C_3A$ (cubic)** | **$C_3A$ (orthorhombic)** | **Quartz** |
| 52.1 | 30.5 | 10.2 | 3.3 | 0.8 | 0.3 |

Table 4



| w/cm = water/cementitious material | 0.557 | | | | 0.483 | | | | 0.426 | | | |
|---|---|---|---|---|---|---|---|---|---|---|---|---|
| f/agr = (cement+fly ash+fine aggregate)/(cement+fly ash+fine aggregate+coarse aggregate) | 0.539 | | | | 0.54 | | | | 0.541 | | | |
| Fly ash [%] | 0% | 20% | 50% | 50% | 0% | 20% | 50% | 50% | 0% | 20% | 50% | 50% |
| fa/agr= Fine aggregate/ fine aggregate+coarse aggregate | 0.462 | 0.460 | 0.459 | 0.459 | 0.449 | 0.448 | 0.446 | 0.446 | 0.437 | 0.435 | 0.432 | 0.432 |
| Paste Volume [l] | 277 | 286 | 301 | 301 | 292 | 303 | 320 | 320 | 307 | 320 | 339 | 339 |
| Cement [kg] | 316 | 253 | 158 | 158 | 363 | 290 | 182 | 182 | 410 | 328 | 205 | 205 |
| Fly ash [kg] | | 63 | 158 | 158 | | 73 | 182 | 182 | | 82 | 205 | 205 |
| Fine Aggregate 1 (#4 - 4.75 mm) [kg] | 696 | 683 | 667 | 667 | 663 | 650 | 631 | 631 | 631 | 616 | 594 | 594 |
| Fine Aggregate 2 (#50 - 0.3 mm) [kg] | 174 | 171 | 167 | 167 | 166 | 163 | 158 | 158 | 158 | 154 | 149 | 149 |
| Coarse Aggregate (1/2" - 12.5 mm) [kg] | 1013 | 1003 | 983 | 983 | 1017 | 1002 | 981 | 981 | 1016 | 1001 | 977 | 977 |
| Water [kg] | 175 | 175 | 175 | 175 | 175 | 175 | 175 | 175 | 175 | 175 | 175 | 175 |
| Admixture 1 (Lignosulfonate) | 0.45% | 0.45% | 0.45% | 0.45% | 0.45% | 0.45% | 0.45% | 0.45% | 0.45% | 0.45% | 0.45% | 0.45% |
| Admixture 2 (Polycarboxylate) | 0.60% | 0.60% | 0.85% | 0.85% | 0.60% | 0.60% | 0.85% | 0.85% | 0.60% | 0.60% | 0.85% | 0.85% |
| Activator (Sodium sulfate) | | | | 1% | | | | 1% | | | | 1% |

Table 5



| Mix ID (1/2/3/4/5) | |
|---|---|
| **Letters and numbers order** | **Description** |
| 1 | W/CM |
| 2 | Cementitious material |
| 3 | Cementitious material percentage |
| 4 | Curing type |
| 5 | Activator |
| **1 - W/CM** | |
| 0.557 | |
| 0.483 | |
| 0.426 | |
| **2 - Cementitious Material** | |
| CE | Cement |
| TP | TP fly ash |
| **3 - Cementitious Material Percentage** | |
| 0 | 0% |
| 20 | 20% |
| 50 | 50% |
| 100 | 100% |
| **4 - Curing type** | |
| L | Lab curing |
| O | Outdoor curing |
| **5 - Activator** | |
| A | Sodium sulfate |

Table 6



| CONCRETE EVALUATION | STANDARD TEST METHOD | | AGE (Days) |
|---|---|---|---|
| Compressive strength | Standard Test Method for Compressive Strength of Cylindrical Concrete Specimens | ASTM C 39 **[28]** | 1, 3, 7, 28, 56, 90, 360 |
| Water permeability | Metodo de ensayo para determinar la permeabilidad del concreto al agua / Standard test method for water permeability of concrete | NTC 4483 **[29]** | 90, 180, 270, 360 |
| Chloride penetration | Standard Test Method for Electrical Indication of Concrete's Ability to Resist Chloride Ion Penetration | ASTM C 1202 **[30]** | 28, 90, 180, 270, 360 |
| Chloride diffusion coefficient | Chloride Migration Coefficient from Non-Steady-State Migration Experiments | NT BUILD 492 **[31]** | 90, 180, 270, 360 |
| Carbonation | Products and Systems for the Protection and Repair of Concrete Structures. Test Methods. Determination of Carbonation Depth in Hardened Concrete by the Phenolphthalein Method | BS EN 14630 **[32]** | 28, 90, 270, 360 |